# Heat shock alters the distribution and interaction of major nuclear proteins—Lamin B with DNA topoisomerase II and chromatin.

## Authors

**Marta Rowińska[1*], Aleksandra Tomczak[1*], Jadwiga Jabłońska[1,2], Aleksandra Zielińska[1], Katarzyna Piekarowicz[1], Magdalena Machowska[1] and Ryszard Rzepecki[1,&]**

*[1]Laboratory of Nuclear Proteins, Faculty of Biotechnology, University of Wroclaw, Wroclaw, Poland, Fryderyk Joliot-Curie Street 14a, 50-383 Wroclaw, Poland*
**[&] Corresponding author:** *ryszard.rzepecki@uwr.edu.pl*
*** Joint first author**
[2]present address: Department of Biophysics and Neuroscience, Wroclaw Medical University, Chalubinskiego Street 3A, Wroclaw, Poland

**Acknowledgment:** Funded by the National Centre for Science (NCN) grant Nr 2016/21/B/NZ4/00541. I would like to thank Prof. Paul A. Fisher (Dept. of Pharmacology, SUNY SB, USA) for allowing me to perform initial studies in his laboratory.

## ABSTRACT

Lamins and topoisomerases play a critical role in the structural support of cell nuclei, in the regulation of chromatin structure, chromatin distribution, topology of DNA, gene expression, transcription, splicing and transport. Here, we report the role of lamins and Top2 during transition from normal conditions (N), in heat shock (HS) and recovery (R) in *Drosophila* since the fly genome contains a single gene for B-type lamin (lamin Dm), for A-type lamin (lamin C) and Top2. Heat shock increases transient phosphorylation of lamin Dm on S25, induces changes in solubility of lamin Dm, Top2, HSF, HDAC1 and HP1 proteins, especially in S2 cells and relocates Top2 and chromatin closer to the nuclear lamina with induction of granular staining for Top2 in Kc, S2 and embryonic cells. Lamin Dm interacts with Top2 protein and HS increases the interaction. *In vivo* photocrosslinking and immunoprecipitation revealed a significant increase in binding to chromatin and nucleic acids upon HS induction for Top2 and lamin Dm. All the detected changes in the properties and location of proteins returned to “normal” after recovery from heat shock. This suggests an important role for lamin Dm, Top2 and their complexes in nuclear functions during HS and recovery. We propose a model in which relocation of Top2 chromatin complexes closer to the nuclear lamina and lamin Dm may help to rearrange the gene expression pattern by tethering HS inactivated genes to nuclear lamina and NPCs which might also help to bind nuclear fraction of non-HS-related transcripts at the nuclear lamina/NPCs area.

## INTRODUCTION

Lamins and topoisomerase II (Top2) have been considered among the major components of karyoskeletal structures since the early 1980s, when commonly used experimental analyses were based on the isolation of the nuclear matrix (NM) or chromosomal/nuclear scaffold structures [1]–[6]. Importantly, heat shock (HS) in mammalian cells has been reported to dramatically increase protein content and affect the composition of NM fractions generated by cell fractionation *in vitro* and sequential extraction [7]. Similar observations have been reported for *D. melanogaster* [8], [9] as well as for the formation of the mitotic chromosome scaffold [10]–[12] and plant nuclear matrix preparations [13], [14]. To date, the biological/biochemical basis for these well-documented and ubiquitous effects of thermal stress has remained relatively unclear.

Lamins are type V intermediate filament proteins that play critical roles in all nuclear functions in metazoans, starting from mechanical and organizational functions supporting the nuclear envelope (NE), nuclear lamina (NL), nuclear pore complexes (NPCs), chromatin structure and subnuclear compartmentalization, as well as their involvement (directly and/or indirectly) in replication, the regulation of transcription, splicing, and transport, and as hubs/platforms for integrating nucleocytoplasmic signaling [15], [16]. Lamins and interacting proteins are also directly involved in the positioning and transport of cell nuclei within cells and tissues as well as in the mechanical properties of cell nuclei, mechanosensing [17] and mechanotransduction of signals from other parts of the cell and the extracellular matrix [18], [19]. All of these functions lamins perform directly or indirectly by forming different protein complexes within different nuclear subcompartments. It has been commonly believed that most of these functions of lamins are regulated by phosphorylation/dephosphorylation at specific, evolutionally conserved sites (with the help of 14-3-3 protein and prolyl-protein isomerase Pin1), which affects particular lamin particle polymerization states, locations, solubility, interactions with other proteins (or protein complexes) and interactions with chromatin components such as histones, nonhistone proteins and DNA [20]–[25].

Typically, metazoan lamins are divided into two types: A-type lamins, which in mammalian somatic cells are represented by lamin A and lamin C proteins derived from alternatively spliced *LMNA* gene, and B-type lamins, represented by lamin B1 and B2 proteins, which derive from separate *LMNB1* and *LMNB2* genes, respectively. Lamin C variant and lamin B3 (from *LMNB2*) are splicing variants synthesized in germline tissues. In *Xenopus* and *Teleostea* fish, there are extra copies of the lamin A and lamin B genes; in *C. elegans,* there is only a single lamin Ce; and in *D. melanogaster*, there are two genes and two lamin proteins: lamin C of the A-type and lamin Dm of the B-type [26], [27]. Lamin Dm is present at all stages of fly development, whereas lamin C protein appears in the late stage of embryogenesis [28]. The latter has all the typical functional protein domains and phosphorylation sites of mammalian lamin C homologs. Fly lamin Dm exists as different isoforms, mostly depending on the phosphorylation pattern [24], [29]. Many different phosphorylation sites can be modified in lamin Dm (for review, see [24], [29]), but previous $^{32}P$ labeling studies have demonstrated that the average

number of phosphorylations per single protein does not exceed 3 moieties [22], [23], [30], [31].

Lamin Dm gene has been cloned and sequenced in 1988, and two transcripts were detected giving rise to a single polypeptide protein which has been named as the lamin $Dm_0$ polypeptide [32]. Lamin $Dm_0$ polypeptide, as newly translated (*in statu nascendi*) form is immediately phosphorylated to lamin $Dm_1$ form. Then, under certain conditions, its phosphorylation(s) generates lamin $Dm_2$ form. The two polypeptides represent the interphase, polymerized lamin Dm fraction. In SDS–PAGE electrophoresis, Lamin Dm fractions usually migrate at different positions and are named $Dm_1$, $Dm_2$ (so-called interphase forms) and soluble mitotic/meiotic isoforms, which are designated $Dm_{Mit}$/$Dm_{Mei.}$ The ratio of $Dm_1$ to $Dm_2$, at least in tissue cultured cells, varies from about 5:1 to 1:2 or higher, depending on many conditions. The mitotic, soluble fraction has been thought to arise, similar to vertebrate lamins, by phosphorylation of at least one of the two Cdk1-specific sites called “mitotic sites” (for review, see [24]). The conversion of lamin Dm polypeptide from $Dm_0$ to $Dm_1$ and $Dm_2$ has been demonstrated during *in vitro* translation experiments coupled with radioactive phosphate labeling, during oogenesis, embryogenesis, under heat shock conditions and in nuclear matrix preparations from heat shocked cells and embryos [24], [29]–[31], [33], [34]. Phosphorylation site mapping with the use of site directed mutagenesis, affinity purified, domain-specific antibodies, monoclonal antibodies ADL84, ADL67 and LC-MS/MS allowed to detect many *in vivo* phosphorylation sites: S19, S25, S45, S595 and T597. For review of the sites and diagrams with the distribution of phosphorylation sites see: [24], [29]). Analyses of lamin Dm with single pseudophosphorylation mutants have demonstrated, that both N and C-terminal “mitotic” Cdk1 sites are necessary for the mitotic lamin Dm disassembly and nucleic acid/chromatin binding in tissue culture model and *in vitro* with T435 (C-terminal Cdk1 site) being also responsible for nuclear transport in fly S2 and HeLa cells. S25 pseudophosphorylation has resulted in mildly disturbed structure *in vitro* and minor mislocatization in S2 and HeLa cells [23]. Interestingly, a single 14-3-3 protein binding motif has been discovered in the lamin Dm head domain (R22PPS) encompassing the S25 site. A similar site has been discovered in human lamin B1 protein (R10MGS). In lamin Dm, this motif has been predicted to be a target for Prolyl-isomerase PIN1 which might provide additional regulatory mechanism for lamin Dm *in vivo*. The absolute importance of the N-terminal lamin Dm fragment for regulation of its properties, partner binding and chromatin interactions has been demonstrated experimentally *in vitro* and *in vivo* (for review see: [24], [29]).

In contrast to lamins, the structural and organizational roles of Top2, especially in interphase cell nuclei, have not been studied extensively. Previous studies of Top2 focused mostly on its enzymatic role in maintaining the proper topology of DNA in chromatin and unwinding during transcription and replication. These findings imply that the role of Top2 in the topology of condensing DNA into mitotic chromosomes involves the resolution of sister chromatids and plays a structural role in the building of mitotic chromosomal scaffolds [35]–[38]. *In vivo*, Top2 is essential during mitosis [39]–[45], where it participates in chromatin condensation [46]–[48] and in the formation of the

mitotic chromosome scaffold [10]–[12]. It is similarly important in meiosis [49]–[52]. As with lamins, a structural role for Top2 in organizing interphase nuclei has been suggested [53]–[56], while the biochemical mechanisms underlying these ubiquitous interactions with RNA and DNA and enrichment in the nuclear matrix upon thermal stress are mostly still elucidated. Interestingly, in studies using *Drosophila* tissue culture models, several *in vivo* binding sites for Top2, as well as the induction of new binding sites to chromatin upon thermal stress, were identified. At least some of them are directly related to so-called heat shock *loci* in *Drosophila* [57].

Our previous studies of Top2 in *Drosophila* together with previous studies from Prof. Fisher lab confirmed the existence of a heterogeneous population of Top2 fractions in fly tissue culture cells and embryos. We detected different populations of Top2 with different solubility properties, interactions, and phosphorylation statuses. We reported a correlation of phosphorylation with the enzymatic activity of the Top2 fractions and reported that the C-terminal Top2 domain was phosphorylated and necessary for interactions with DNA/RNA and the regulation of activity [58]. It was demonstrated that during mitosis, there are two distinct populations of Top2 in cells: one associated with mitotic chromosomes and the second dispersed throughout the cell. We also demonstrated that Top2 binds to DNA and RNA *in vivo* during interphase and mitosis and that the critical region for binding lies within 200 amino acid residues of the C-terminal Top2 protein [58].

In the case of fly lamins, we previously discovered that lamin Dm does bind *in vivo* to DNA and RNA during interphase but not during mitosis, whereas lamin C did not bind to nucleic acids at all in our tests [59]. Like mammalian lamins, fly lamins undergo specific phosphorylation/dephosphorylation during the cell cycle *in vivo* [24], [30]. Analyses of the function of single phosphorylation sites in lamins via pseudophosphorylation mutants demonstrated that single phosphorylation on S37 (Cdk1-N-terminal site) on lamin C induces solubility, whereas for lamin Dm, both N-terminal and C-terminal Cdk1 mitotic sites and, to a lesser extent, S25 increase solubility [23]. All single pseudophosphorylation lamin mutants tested, with the exception of lamin C S37E (the N-terminal Cdk1 site), bound to decondensed chromatin in an *in vitro Xenopus* assembly system. The expression of the mutants in the insect Kc cell line and HeLa cells resulted in an atypical distribution (partially cytoplasmic, intranuclear diffuse, and decreased presence at NL) for lamin Dm single mutants: S45E, T435E (N- and C-terminal Cdk1 sites, respectively) and, to a lesser extent, S595E, which indicates a correlation between phosphorylation, solubility, intracellular distribution, and DNA/chromatin binding [24]. These findings support the hypothesis that the properties of lamins are dependent on their phosphorylation pattern.

*Drosophila melanogaster* tissues, especially salivary glands with polytenic nuclei, together with cultured cells, such as Kc and S2, have been widely used as important models for studies of cell nuclear functions and chromatin structure. The initial attempts at resolving the architecture of skeletal structures of the cell nucleus as well as

chromatin composition and organization within karyoskeletal structures (when the terms “nuclear matrix/chromosomal scaffold”, “nuclear lamina” or “SAR/MAR DNA” have been introduced) have also been performed very frequently in the fruit fly model [3]–[6], [60]–[64]. The fly model has also been useful in the identification of lamins and Top2 as major karyoskeletal and nuclear matrix/chromosomal scaffold proteins as well as their content in karyoskeletal fractions. It has been also believed that their properties depend on the preparation methods and conditions of the initial biological material used for preparation. For example, pretreatment of fly material at 37°C or mammalian material at 42°C (heat shock) resulted in more lamins and Top2 in prepared karyoskeletal structures, whereas RNAse treatment during the procedure resulted in the almost complete loss of karyoskeletal proteins, including lamins and Top2, from such preparations [8]–[12], [33], [65]. Similar differences in the protein composition of NMs/NSs prepared *via* different methods have also been detected in plants [13], [14]. Therefore, our and others scientific interests have been focused on the role and properties of lamins, and Top2 in the fly model, and demonstrated *in vivo* interactions of lamins and Top2 with both DNA and RNA and that they interact mostly with AT-rich regions of DNA. Lamin Dm and Top2 have been reported to exist in cells in different complexes with different posttranslational modifications [66]. Therefore, an exploration of the role of lamins and Top2 in the regulation of chromatin structure, gene expression and chromatin binding under normal conditions and during heat shock is needed, for at least several reasons.

Firstly, B-type lamins have been involved, together with A-type lamins and interacting proteins, in chromatin organization forming LADs domains at the nuclear lamina and nucleoli (nLADs). B- and A-type lamins form a hub or docking platform for integration of signaling pathways, including mechanosensing and mechanotransduction, between cell nucleus, cytoplasm and extracellular matrix [17]–[21]. Nuclear lamina with lamins and lamin-interacting proteins support proper organization of entire chromatin domains, also formed by other chromatin proteins [29], [67]–[69]. Top2 has been involved in chromatin organization and topology of DNA and chromatin during interphase affecting gene transcription profile. Top2 has been shown to be essential at mitosis and in the formation of chromosomal scaffold structure and skeletal structure of cell nucleus. Not to forget reports on identification new, induced by heat shock binding sites *in vivo* on many loci including heat shock loci [66], [70], [11], [53], [71]–[73]. Therefore, the heat shock induced rearrangement of global gene expression profile should involve also lamins and Top2 protein [74]. That is why we have decided to look into the lamins and Top2 behavior during heat shock. Thus, we have launched the project to reveal molecular mechanisms regulating lamins and Top2 interactions upon stress induction. Here we report the experimental data from the first part of the project.

In this work we analyzed the effects of thermal stress on lamin Dm, lamin C, Top2, HSF, HDAC1 and HP1 localization, properties and interactions in Kc and S2 cells, embryos and in larvae upon heat stress induction and recovery. We used two different cell lines because they have been selected from different embryonic stages of development, therefore they differ significantly in gene expression profile and in lamins

expression [75]. S2 cell line expresses only lamin Dm while Kc cells express both lamin Dm and lamin C. Please note that early embryos tissues do not express lamin C and the first embryonic cells expressing lamin C are aenocytes and then later on are hindgut and posterior spiracles cells (Stage 11/12; about 9 hours). Ubiquitous lamin C expression takes place at the end of embryogenesis while lamin Dm protein and transcripts are present in embryos from the very beginning (maternally provided) and their expression continues from zygotic lamin Dm genes.

In our study we demonstrate the significant, reversible increase in lamin Dm S25 phosphorylation upon heat shock induction (HS) and recovery (R) and significant changes in solubility of lamin Dm, Top2, HDAC1, HSF proteins upon HS induction. We demonstrate the changes in distribution of top2 between control cells (N) and during HS induction. We report for the first time that lamin Dm and top2 protein interact in normal conditions and that this interaction increases during HS. We also report that lamin Dm and top2 colocalizes with top2 on chromatin during normal conditions and colocalization increases upon HS induction. We also report that HS increases *in vivo* lamin Dm and Top2 binding to nucleic acids. All of the demonstrated HS-associated effects are reversible upon cells and embryo recovery from heat shock.

## MATERIALS AND METHODS

### Antibodies

The affinity-purified rabbit anti-lamin Dm and domain-specific rabbit anti-Top2 antibodies used in this study have been previously described [58]. Guinea-pig anti-LBR was a generous gift from Georg Krohne, University of Würzburg, Germany [76]. The mouse monoclonal antibodies ADL67.10 (anti-lamin Dm, specific for the lamin rod domain fragment), ADL84.12 (anti-lamin Dm, specific for the nonphosphorylated S25 residue), and LC28.26 (anti-lamin C) were obtained from the Developmental Studies Hybridoma Bank (DSHB). Mouse and rabbit anti-α-tubulin antibodies were obtained from DSHB (clone 12G10) and Thermo Fisher (#PA5-29444), respectively. The monoclonal rat anti-Hsp70 (heat shock protein 70 kDa) antibody (NBP2-59342) and rabbit polyclonal antibody against histone deacetylase I (HDAC1; #NB500-124) were obtained from Novus Biologicals. The rabbit polyclonal antibody anti-heat shock factor (Hsf) was custom-made by Thermo Scientific. Additional immunofluorescence staining was performed with rat anti-Hsp90 (heat shock protein 90 kDa; #ab13494) and rabbit anti-Pol2PS5 (RNA polymerase II, phosphorylated at Ser5; #ab5131) from Abcam and rabbit anti-HP1 (heterochromatin protein 1; #NB110-40623) from Novus Biologicals. The secondary antibodies used were from Jackson ImmunoResearch. HRP-conjugated anti-mouse (#715-035-151), anti-rabbit (#111-035-144), and anti-rat (#712-035-153) antibodies were used to visualize antigens on the membranes after immunoblotting. The secondary anti-mouse antibodies used for immunofluorescence were conjugated with TRITC or DyLight649 (#715-025-151, #715-495-150). The anti-rat antibodies were

coupled to TRITC (#712-025-153), while the anti-rabbit antibodies were conjugated with Alexa488 (#711-545-152).

### *Drosophila melanogaster* embryos and cell cultures

The *D. melanogaster* Oregon R-P2 strain (RRID:BDSC_2376) was obtained from Bloomington Drosophila Stock Center, Bloomington, USA (NIH P40OD018537). The embryos were collected in special egg-laying cages. Flies were transferred from standard media (6,25% w/v corn grits, 3,13% w/v corn flour, 6,25% w/v sugar, 12,5% w/v yeast and 0,5% w/v bacteriological agar) to cages with embryo assembly media (20 ml apple juice, 10 ml cherry syrup, 10 ml water and 2,5 g sugar, 1,6 g bacteriological agar, coated with yeast paste). The flies were allowed to lay embryos for 11 hours, after which a 1 hour heat shock at 37 °C was performed. The ages of the analyzed embryos ranged from 1 hour to 12 hours. Kc cells (ECACC #90070550) and S2 cells (Drosophila Genomics Resource Center; Stock 6; https://dgrc.bio.indiana.edu//stock/6; RRID:CVCL_TZ72, a kind gift from the Department of Cytobiochemistry, University of Wroclaw, Poland) were cultured in Schneider's Drosophila Medium (Gibco #21720024) supplemented with 10% fetal bovine serum (Sigma #7524) and 1% antibiotic-antimycotic mixture (Gibco #15240062) at 23 °C (N) without additional $CO_2$.

### *Preparation of D. melanogaster* embryos and cell lines for Western blot

The embryos were rinsed with water to special strainers with a nylon filtration fabric NITEX (40 µm). The chemical dechorionation procedure was carried out using 5% sodium hypochlorite. Then, the embryos were washed with a washing buffer (5 mM NaCl, 20 mM Tris-Cl pH 7,5, and freshly added protease and phosphatase inhibitors). The embryos were then processed according to specific protocols for particular experiments.

The cells were plated on a 10 cm culture dish 24 hours before each experiment. The cells were collected by gently scratching the cells from the culture plates and pelleting them via centrifugation. The cell pellets were resuspended in Laemmli loading buffer and heated at 95 °C for 10 minutes before WB analysis. For heat shock induction, the material (embryos, larvae and cells) was shifted to 37 °C and maintained at this temperature for 1 h (or a certain amount of time, as indicated in the text). Recovery (R) was initiated by a return to 23 °C for an additional 6-, 24-, 48-, or 72- or 96 h. Unless stated otherwise for heat shock induction embryos and larvae were shifted to 37 °C
For 1 h followed by 4h incubation (Recovery (R) time) at 23 °C.

### Western blot analysis

Proteins were separated on polyacrylamide gels (with concentrations ranging between 7% and 12% depending on the experiment) according to Laemmli [77] and then electrophoretically transferred to nitrocellulose membranes according to Harlow and Lane, 1988 [78] (0,45 µm; Amersham Protran) via the Bio-Rad Mini Trans-Blot Cell Set. To estimate protein sizes, a prestained protein ladder from ThermoFisher (#26616) was used. After 1 h of blocking with 5% nonfat milk in PBST (phosphate-buffered saline (PBS), 0,075% Tween-20), the membrane was incubated with primary antibodies

overnight at 4 °C, washed three times with PBST and incubated with secondary antibodies conjugated with HRP for 1,5 h at RT (room temperature). Proteins were detected by using SuperSignal™ West Pico PLUS Chemiluminescent Substrate (Thermo Fisher #34580) or Clarity Western ECL Substrate (Bio-Rad #1705061). Images were acquired and quantified via the ChemiDoc MP Imaging System (Bio-Rad) and the software Image Lab V5.2 (Bio-Rad).

When reactivity is visualized colorimetrically, calf alkaline phosphatase-conjugated goat anti-IgGs antibodies and/or horseradish peroxidase coupled with donkey anti-IgGs with proper single or both substrates are used (Jackson ImmunoResearch).

When Western blots were performed in some co-IP experiments for lamins and Top2, also with BrdU and/or BrdC labeling, UV crosslinking and radioactive $^{32}P$ labeling, reactivity was visualized colorimetrically for both proteins simultaneously using secondary IgGs coupled with horseradich peroxidase for one antigen and secondary IgGs coupled with alkaline phosphatase (typically: goat anti rabbit IgGs-phosphatase for Top2 visualization and goat anti mouse-alkaline phosphatase for lamin Dm visualization) with proper substrates with different colours. As a control for these IP and co-IP experiments isolated IgG fraction from pre-immune rabbit serum or control mouse IgG fraction were used.

**Immunofluorescence**

The cells were cultured on gelatin-coated cover slides for 24 h and heat shocked, if necessary, before fixation. The cells were fixed with 4% paraformaldehyde, permeabilized with 0,5% Triton X-100 in PBS and blocked with 5% FBS in PBS. The cells and embryos were processed as described previously [59], [79].

Before fixation, the embryos were subjected to chemical dechorionation (3 min, 5% sodium hypochlorite) and then rinsed with water. Typically, 100 µl of packed embryos were fixed with 4% PFA (300 µl) with heptane (1 ml) at RT for 20 min. After incubation, the fixative phase was replaced with 1 ml of methanol, the embryos were washed twice with PBS and then hydrated with PBS containing 0,1% Triton X-100 for 30 min at RT. Permeabilization was carried out for 30 min in PBS with 0.5% Triton X-100 at RT with stirring. Finally, the embryos were washed with PBS and stained as described below.

The cells and embryos were subsequently stained with primary antibodies overnight at 4 °C and then with secondary antibodies at room temperature (RT) for 1,5 h. Embryos of stage 10-12 are presented in Figure 3. The ratio of peripheral located Top2 to all visible nuclei was counted. Irregularly stained/showing lack of signal in nuclei center cells were counted manually and represented in relation to all visible cells, in both (N, HS) conditions. The significance of differences between group counts was determined with chi-square statistical testing. An identical method was used for chromatin/DAPI staining relocation into the periphery.

PLA staining with the Duolink PLA Multicolor Reagent Pack (Sigma–Aldrich, #DUO96000) was performed according to the manufacturer's instructions. Primary

antibody incubation was performed for 16 h at 4 °C, after which the slides were washed with PBS and incubated with secondary antibodies in PBS for 1,5 h at RT. The slides were washed with PBS and mounted with VECTASHIELD medium supplemented with DAPI. PLA staining was performed on Kc cells and third-instar larvae (the smears were prepared from larvae and processed in the same way as the cells). Prepared samples were stained according to the manufacturer's protocol. For statistical quantification, the number of visible PLA-stained dots/clusters were divided by number of cells (nuclei=cell: based on DAPI staining).

Microscope images were collected with a Leica SP8 confocal microscope and adjusted with the Fiji image processing package.

## Solubility assay

### Kc cells and S2 cells

The cells were plated 24 hours before the experiment (2,5 × $10^6$ cells/ml). After heat shock induction, the cells were scratched from the plates, transferred to 15 ml tubes, collected by centrifugation at 500 × g for 5 minutes and washed with PBS. The cell pellets were suspended in extraction buffer (5 mM $MgCl_2$, 50 mM NaCl, 50 mM Tris-HCl pH 7,5, 250 mM sucrose, 0,1 M EDTA, 1% Triton X-100 and freshly added protease and phosphatase inhibitors). After mechanical homogenization, the prepared lysate was incubated for 20 minutes on ice (control - the fraction of the cell lysate was collected before further steps). Then, centrifugation was performed (10 000 × g, 10 min, 4 °C), and the supernatant was collected (fraction of proteins soluble in 50 mM NaCl). The pellet was resuspended in the same buffer as above but with 150 mM NaCl, incubated for 20 min on ice, and then centrifuged, and the next supernatant fraction was collected (soluble in 150 mM NaCl). Furthermore, the 500 mM NaCl extraction buffer was used for extraction. The collected samples were boiled in denaturing buffer (5% DTT and 40 mM DTT) for 10 min at 96 °C and prepared for SDS–PAGE in standard Laemmli loading buffer. The application of each sample prepared in this manner, irrespective of the fraction type, was conducted at a final volume of 10 µl on the gel.

### Embryos

The collected and washed embryos were suspended in extraction buffer (the same as in the cell section) at a ratio of 25 mg of embryos to 125 µl of buffer. The next steps of extraction were carried out analogously to those described above.

## Statistics

Data obtained from the measurements of band mean intensities were statistically analyzed between samples maintained under normal conditions (N, 23°C) and after heat shock induction (HS, 1 h, 37°C). For each fraction (lysate, 50 mM, 150 mM, and 500 mM), independent comparisons were performed using the Student's t-test. The analysis was based on mean values calculated from three biological and at least four technical replicates.

## RNA extraction and first-strand cDNA synthesis

Semi-adherent Kc cells were plated at a density of 2,5 × $10^6$ cells/ml in Schneider medium on a 6 cm cell culture plate (in total, 1,5 × $10^7$ cells). After 24 h, the medium

was aspirated, and the cells were washed once gently with PBS. Then, the first lysis buffer from the Universal RNA Purification Kit (Eurx) was added, and all further procedures were performed following the manufacturer's protocol. DNAse I (Eurx) treatment was performed. The RNA concentration and purity were evaluated with a NanoPhotometer® N60 (IMPLEN). RNA samples with an absorbance ratio of A260/280 over 2,2 and A260/230 over 2,2 were used for further analysis. The quality of the RNA samples was verified via 1% native agarose gel electrophoresis.

Single-stranded cDNA was synthesized from 2 µg of total RNA in a final volume of 10 µl. For this purpose, the Maxima First Strand cDNA Synthesis Kit for RT–qPCR (Thermo Scientific) was used, and the manufacturer's instructions were followed. cDNA was stored at −20 °C for future use.

Three biological replicates were used for RNA extraction and cDNA synthesis from all the samples.

## Real-time quantitative PCR analysis

qPCR was performed using Power SYBR Green Master Mix (Applied Biosystems). All reactions were performed under the following conditions: 1) UDG activation at 50 °C for 2 min, 2) Dual-Lock DNA polymerase at 95 °C for 2 min, and 3) 40 cycles of denaturation and annealing/extension at 95 °C for 1 s and 60 °C for 30 s. The specificity of the reaction was verified by melting curve analysis and agarose electrophoresis of the PCR products. All the qPCR experiments were performed via the QuantStudio™ 5 Real-Time PCR System. The sequences of primers used are listed in Supplementary Table 1.

For each well of the plate, the threshold crossing value (Ct) was calculated via the thermocycler manufacturer software (Quant Studio Design and Analysis). Further analyses were carried out via the comparative Ct method. The values were normalized to the most stable gene in the dataset. Differences between the N and HS groups were statistically analyzed via Student's t test.

## Photocrosslinking and $^{32}$P-end-labeling of co-immunoprecipitated nucleic acid

### BrdU incorporation in Kc cells

For routine 5-bromo-2-deoxyuridine (BrdU) incorporation, which was quantified with an anti-BrdU monoclonal antibody as previously described [59], 200 ml of exponentially growing cells (1,2-1,8 × $10^6$ cells/ml) were incubated with 20 µM BrdU and maintained in culture for an additional 26–27 hours [59]. Similarly, 5-bromo-2-deoxycytidine (BrdC) incorporation was achieved.

### Cell fractionation of $^{32}$P-labeled and UV-crosslinked cells

Cell fractionation was performed according to [58]; see also [55]. In brief, the cells were harvested via centrifugation and washed with PBS. Lysates were prepared via a Dounce homogenizer, and the homogenates were filtered and centrifuged (10000

× g, 10 min) to obtain fractions labeled P-10 and S-10 (pellet and supernatant, respectively). The obtained supernatant was then centrifuged (13000 × g, 60 min) to obtain the P-130 fraction.

***In vivo photoc*rosslinking**

*In vivo* photocrosslinking was performed as described previously [58], [59]. A hand-held lamp (UVGL-58, UVP Inc., San Gabriel, CA) emitting 366 nm light was used. All quantities refer to 200 ml of cell culture starting material. For the experiments with distamycin and chromomycin, cell culture was supplemented with the drugs (50 μM distamycin A3 and/or chromomycin (Sigma)) 24 hours before harvesting. For heat shock experiments, before cell harvesting cells were divided into three fractions: N, HS and Recovery, processed as described above for heat shock induction and recovery than harvested, washed and resuspended in PBS for the rest of the photocrosslinking procedure.

The cells were harvested, washed and resuspended in 8 ml of PBS, as described previously and subjected to illumination with 366 nm light as described above.
For heat shock experiments, before cell harvesting cells were divided into three fractions: N, HS and Recovery, processed as described above for heat shock induction and recovery than harvested, washed and resuspended in PBS for the rest of procedure.

**Immunoprecipitation and $^{32}$P-end-labeling of coimmunoprecipitated nucleic acid**

The entire procedure has been described previously [58], [59]. After *in vivo* photocrosslinking, the cells were lysed for cell fractionation or lysed directly and denatured by the addition of SDS and DTT (final concentrations of 5% and 20 mM, respectively); after the addition of SDS and DTT, the samples were boiled for 10 min. Typically, approximately 6 × $10^8$ cells were harvested, resuspended in 1,5 ml of PBS, lysed and either denatured immediately or fractionated and then denatured by the addition of a solution containing 10% SDS and 40 mM DTT. Whole-cell lysates and/or subcellular fractions prepared in this way were stored at -20 °C until use. The samples, each derived from approximately 1,5 × $10^7$ cells, were thawed by boiling for 10 min and cooled to room temperature, after which trichloroacetic acid (TCA) was added to a final concentration of 10%. The samples were then incubated for 10 min at room temperature, and the precipitated proteins were collected *via* centrifugation at room temperature for 10 min at 10,000 × g. The supernatant was discarded, 5 μl of 1,5 M Tris-HCl (pH 8,8) was added to the protein pellet, and the pellet was dissolved in 200 μl of a solution containing 20 mM Tris-HCl (pH 8), 150 mM NaCl, 0,1% Triton X-100 and 0,02% SDS (Buffer IPA). Immediately before use, Buffer IPA was supplemented with 2.5 mM $CaCl_2$, 0,5 mM PMSF, 1 mM TPCK, 1 mM TLCK, 1 μg/ml leupeptin and 1 μg/ml pepstatin. Unless otherwise indicated, 5 μl of micrococcal nuclease (680 μg/ml; Boerhinger) was then added, and the samples were incubated for 60 minutes at 37 °C.

Immunoprecipitation was performed as modified by Rzepecki et al. [58]. Briefly, for this purpose, protein A-Sepharose (Pharmacia, Piscataway, NJ) conjugated with antibodies was used (2–4 μg of purified IgG was used per 50 μl of beads and incubated

for 90 min at 37 °C). The supernatant was subsequently centrifuged, and the buffer with unbound antibodies was discarded. The prepared beads were incubated with the prepared lysates for 90 min at 37 °C. The beads bound to the IgG and antigen (immunoprecipitate) were recovered via centrifugation and washed three times with 350 µl each of Buffer IPB, followed by three identical washes with Buffer IPA [33], [59].
After the final wash in Buffer IPA, the washed immunoprecipitate was resuspended in 80 µl of 1.5× concentrated T4 polynucleotide kinase buffer (New England Biolabs, Beverly, MA). To this resuspended immunoprecipitate was added 1-2 µl of [γ-$^{32}$P]ATP (4500 Ci/mmol; 10 µCi/µl; ICN Pharmaceuticals, Costa Mesa, CA) and 5 units of T4 polynucleotide kinase (New England Biolabs, Beverly, MA). No unlabeled ATP was added. $^{32}$P-labeling with T4 polynucleotide kinase was for 30 minutes at 37°C. After this incubation, the $^{32}$P-labeled immunoprecipitates were washed three times with 350 µl of Buffer IPB and finally resuspended in 45 µl of 2.5× concentrated standard SDS-PAGE loading buffer, followed by electrophoresis on an SDS-7% polyacrylamide gel and electrophoretic transfer to nitrocellulose for autoradiography or phosphorimager (Molecular Dynamics 445 SI) and immunoblot analyzes.

**Nucleases and nuclease digestion**

Nuclease and nuclease digestion were carried out exactly as described previously [59]. To study the sensitivity of $^{32}$P-labeled nucleic acid photocrosslinked to Top2, nuclease digestions were performed for 30 min at 37 °C with final concentrations of 66 µg/ml DNase I and 60 µg/ml RNase A. All nuclease digestions were performed in a solution containing 20 mM Tris-HCl pH 8, 150 mM NaCl, 0,1% (v/v) Triton X-100 and 0,02% (w/v) SDS (Buffer IPA) supplemented with 5 mM $MgCl_2$ and 2,5 mM $CaCl_2$.

**Quantification by scanning densitometry**

Unless stated otherwise, immunoblots and autoradiograms (or PhosphorImager scans) were quantified via an LKB Mltrascan XL laser densitometer (LKB Instruments Inc., Gaithersburg, MD).

## PFA crosslinking and co-immunoprecipitation

**Cell collection and crosslinking**

HS induction and cell collection were performed in the same manner as for the solubility assay. Pelleted cells (25 × $10^6$) were resuspended in 2 ml of crosslinking reagent (1% paraformaldehyde) and incubated for 7 min with gentle rotation on a rotary agitator at RT. After incubation, the cells were immediately centrifuged for 3 min at 1000 × g at RT. Pelleted cells were resuspended in 1 ml of 125 mM glycine solution (to quench the PFA and terminate the crosslinking process), incubated on a rotary evaporator for 5 min and then centrifuged at 4 °C.

Next, the cells were washed with cold PBS supplemented with protease and phosphatase inhibitors, centrifuged, resuspended in lysis buffer (50 mM Tris-Cl pH 7,5; 150 mM NaCl, 1 mM EDTA, 1% Triton X-100, 0,1% SDS, Halt Protease and Phosphatase Inhibitor Cocktail from ThermoScientific) and transferred to 1,5 ml tubes.

Mechanical homogenization was performed with plastic pestles followed by incubation for 20 min on ice. The prepared lysate was sonicated (Bandelin Sonoplus Mini 20) for 25 minutes at 90% amplitude with a pulse (30 sec ON–OFF cycles). The sonication method has been optimized to obtain a homogenous trace of DNA <500 bp with no protein loss. After sonication, the lysate was centrifuged at 8000 × g for 10 min at 4 °C. The supernatant was collected for further steps.

**Co-immunoprecipitation**

In accordance with the manufacturer's instructions, 25 µl of Pierce Protein A/G Magnetic Beads (ThermoScientific # 88802) per sample was used. Initially, 200 µl of cell lysate with 10 µg of primary antibody (anti-lamDm, anti-Top2) was rotated for 1,5 h at RT (volume adjusted to 500 µl with lysis buffer). The antibody-lysate mixture was subsequently transferred to previously washed beads and incubated for 1 h at RT with rotation. The beads were collected with a magnetic stand (Thermo Fisher #CS15000) between each washing step. Before the first wash, the flow-through fraction (excess unbound antibodies and lysate) was collected for further analysis. Elution was performed by adding 100 µl of Laemmli buffer and heating the samples for 10 min at 96 °C. After cooling, the supernatant was collected.

The negative control in the experiment consisted of identically treated samples, with the exception of the antibodies; as an isotype control, normal polyclonal rabbit IgG was used (R&D Systems, #AB-105-C).

A total of 10 µl of each sample was loaded onto a polyacrylamide gel together with the corresponding controls (input, negative control, and flow-through fractions), and proteins were detected by immunoblotting via primary antibodies (anti-lamDm, anti-Top2, and anti-LC28.26), followed by the addition of HRP-conjugated anti-rabbit or anti-mouse IgG (described in the *Antibodies* section).

**Western blot quantification of protein levels**

Western blot membranes were imaged using Image Lab 5.2.1 software (Bio-Rad Laboratories). Densitometry analysis of protein bands was performed using the Volume Analysis tool. The area of the stained band was marked with a rectangle (the areas were identical for each band on the membrane). Quantification was based on the Mean Value (Int), which represents the mean intensity of all pixels within the defined volume boundary.

For protein level estimation: each nitrocellulose membrane contained a molecular weight ladder and three independent biological replicates, with each replicate comprising four experimental conditions: N (control), HS (heat shock), R (recovery), and NR (control for recovery). To enable the detection of multiple proteins with different molecular weights on the same membrane, membranes were cut horizontally into strips corresponding to the expected molecular weight ranges of the target proteins. This allowed for separate antibody incubations and staining of different proteins from the same membrane, ensuring consistent sample loading across targets.

The experiment was conducted with at least three technical replicates per protein, corresponding to three independent membranes (n = 9). For N = 12, data were

obtained from three biologically independent experiments, each analyzed in four replicates. If staining quality for the bands or the membrane region corresponding to a given biological replicate was compromised, that biological replicate from the affected technical replicate was excluded from further analysis.

For each protein of interest, densitometry values were normalized in two steps: Normalization to housekeeping protein: The Mean Value (Int) of the target protein was divided by the corresponding Mean Value (Int) of the housekeeping protein α-tubulin from the same lane to correct for loading and transfer variability.

Normalization to the mean of the biological replicate: To account for membrane-specific variability, each normalized value was further divided by the mean of all four conditions (N, HS, R, NR) within the same biological replicate. This allowed for comparison of relative expression changes across conditions, independent of overall signal intensity on a given membrane.

Normalized data were exported to GraphPad Prism 10.6.1 for statistical analysis. Ordinary one-way ANOVA was performed to assess differences between experimental conditions. Statistical significance was defined as $p < 0.05$. Non-significant results were denoted as ns ($p > 0.05$).

For the solubility assay, each fraction (lysate, 50 mM, 150 mM, 500 mM) was analyzed in three biological replicates and at least three technical repetitions. For each fraction, the three biological replicates were loaded on the same gel, and the intensity of individual bands was normalized to the mean densitometric signal within the respective fraction. Values in a given fraction according to a given test condition (N or HS) were then averaged, and the standard deviation was calculated. It should be noted that this method only allows for comparisons within a given fraction (N vs. HS), as each fraction must be analyzed separately due to the method of densitometric quantification. For the purpose of this study, the term 'biological replicates' refers to separate cell populations and fractionations. The technical repetition is defined as the repeated measurements (WB analysis) of the same biological sample.

**Statistical analysis and data presentation**

Statistics (Fisher's exact test and t-test unless indicated otherwise in the text) were calculated via Microsoft Excel. The quantified data were plotted via GraphPad Prism 8.0. The details of the experimental replicates and statistical analysis are described in the corresponding figure legends. Independent experiments mentioned in the figure legends are biological replicates.

**Data availability**

All the data associated with this manuscript have been deposited on the Faculty of Biotechnology, University of Wroclaw server. Please contact the Authors for address, login and password details.

## RESULTS

### Induction of heat shock and recovery in *Drosophila melanogaster* tissue culture cells and embryos

For this study, we chose a fruit fly cell culture model system based on Kc and S2 cells, and whenever possible, we also tested embryos and larvae at the desired stages. Lamin Dm is present in both cell types, whereas lamin C is present only in Kc cells. In embryos, lamin C protein starts to be expressed firstly in aenocytes and then hindgut (Stage 10-12; about 9 hours). First, we tested the conditions and reversibility of thermal stress induction (heat shock, HS) and recovery time (R) using inducible Hsp70 protein as the HS marker. Panels 1A and 1B from Figure 1 demonstrate that HS induction can be easily detected by IF in Kc and S2 cells, and that in both cell lines cells fully recover from the HS (Figure 1A and B). Staining for Top2 protein revealed the population of cells in HS with induced modified distribution of protein which disappears during recovery. Arrows and arrowheads point out cell nuclei with two most frequent types of phenotype detected in cells during heat shock: sublaminar and granular staining for Top2 and/or one or few bigger granules, respectively. Both cell lines demonstrate similar Top2 phenotype in cells during HS.

The analysis of the time frame of Hsp70 protein induction detected by WB in Kc and S2 cells indicated that S2 cells recover faster from HS, as judged by Hsp70 protein level – after 6h recovery, most of the protein band disappeared (Figure 1C). Kc cells after 6h retained at least the same, or increased, level of Hsp70 protein but in both cell lines more than 95% of protein disappeared after 24 hours. Taking into account the doubling time for both cell lines (24-32h, as judged by BrdU incorporation [59]), this strongly suggests fast degradation of the protein but not dilution. Fast disappearance of Hsp70 IF signal in early embryos during recovery time (4h) (Supplemental Figure 1) suggests similar properties in this respect of S2 cells (early embryonic origin) and early embryos itself. The HS causes the increased expression of typical, marker HS-inducible genes, including *Hsp70* in Kc cells at 15, 30 and 60 min respectively demonstrating that 1 hour induction fully activates marker HS genes (Figure 1D). Please note that Kc and S2 cells differ in the level of transcripts of the marker HS genes (Figure 2 B). The induction of Hsp70 protein was also reversible in embryos which was shown by IF staining (Supplementary Figure 1). Taken together, these findings clearly indicate that the HS effect in all of the experimental models is typical and fully reversible. Additionally, in cellular model we detected induced, reversible Top2 phenotype induction.

On the basis of the remaining levels of Hsp70 proteins in the WB experiments, similar to those shown in Figure 1C, we chose 48 and 72 hours as the best recovery times for S2 and Kc cells, respectively, while as the optimal time for HS induction, we set 1 hour. Since HS affects the expression of many genes [80], [81], we tested several genes or their combinations as references for RT–qPCR analyses under normal (N) and heat shock (HS) conditions. On the basis of our analyses using geNorm , the most

stably expressed transcripts seem to be the ribosomal RNAs, actin5C and tubulin84B when the HS and N groups were compared (Supplementary Figure 2B).

Considering the above, we chose 18S/28S ribosomal RNA, actin5C and tubulin84B as references for RT–qPCR. Please note that we have detected the transcript for lamin C in S2 cells, but this signal was visible only after at least 7 cycles after the signal from Kc cells transcript (Suppplementary Figure 2A) and on WB we did not detect lamin C protein in S2 cells (not shown). These data are fully compatible with knowledge about lamin C expression in Kc cells and its lack in S2 cells (Supplementary Figure 2A and Figure 2A).

Quantitative analyses of lamin Dm, lamin C, Top2 and Hsf transcripts via RT-qPCR revealed that their transcript levels do not change significantly after heat shock, however, for lamins and Top2, we observed a decreasing trend, whereas Hsf increased in both cell lines (Figure 2A). Comparison of the induction of typical HS-inducible genes revealed that stress induction of their transcripts was slightly lower in S2 cells than in Kc cells (Figure 2B).

**Heat shock affects the phosphorylation pattern of lamin Dm but does not affect the total protein level**

We analyzed the levels of selected proteins during HS induction and recovery in Kc and S2 cells *via* western blotting. For Kc cells, we did not observe any statistically significant changes in the levels of Top2, both lamins, HDAC1 or Hsf (Figure 2C, WB). Please note the modified mobility of the Hsf protein band in both cell lines (Figure 2C and 2D), which is phosphorylated upon HS [82]. HS induction in S2 cells (no lamin C protein) significantly increased the level of Top2 and Hsf but not HDAC1 levels. Please note a significant decrease in Top2 and lamin Dm levels upon recovery in both cell lines (Figure 2C and 2D).

Interestingly, HS and recovery induced significant changes in the proportions of lamin Dm forms, inducing the changes in proportion of lamin Dm bands which suggest the conversion of lamin $Dm_1$ (lower band) into the lamin $Dm_2$ form, as shown by blots stained with the rabbit polyclonal antibody anti-lamin Dm in Kc cells (Figure 2C; WB, lamin Dm total) and less visibly in S2 cells (Figure 2D; WB, see also: Figure 5F, magnification in Figure 5G). Please see also Western blots from Supplemental Figure 5, total lamin Dm, for visible two lamin bands and their proportions in fractions from control and heat shocked cells.

Since this effect is reversible after recovery time, we suggest that it is a HS-specific induction of lamin Dm modification. It has been reported previously that the conversion of fly lamin from $Dm_1$ to $Dm_2$ is correlated with the phosphorylation of the N-terminal fragment and at least one phosphosite was identified *in vivo* and mapped as S25 [34]. To confirm the conversion of lamin Dm upon HS induction by phosphorylation at N-terminal S25, we used the monoclonal antibody ADL84, which has been demonstrated to be highly specific for the N-terminal lamin Dm fragment and recognizes only lamin Dm when S25 is not phosphorylated. Notably, phosphorylation of S25

abolishes recognition by these antibodies in vitro and restore of recognition by this ADL84 antibodies when Western blots with lamin Dm are treated with phosphatase before antibody ADL84 staining [34]; see also [30]. Using this antibody for western blotting, we identified a single band, and its optical density decreased upon HS and returned to normal levels upon recovery in Kc cells and to the lesser extent in S2 cells (WB in Figure 2C and Figure 2D, respectively). Densitometry analyses of western bloting stained with antibodies ADL84 (illustrated by the diagram in Figure 2C and 2D) indicated that the HS induced decrease in lamin Dm not phosphorylated at S25 and its full recovery in Kc cells (no difference between N and R conditions) . Similar analyses performed on S2 cells *via* WB are illustrated in Figure 2D and associated diagrams from densitometry analyses and demonstrated no significant differences but similar trend in ADL84 staining during HS and recovery. Since the phosphorylation of lamins can affect their properties and interactions, we investigated the phosphorylation of lamin Dm more deeply. Similar western blot experiment and analyses with direct comparison of "total" lamin Dm fraction staining with polyclonal, affinity purified antibodies and ADL84 antibodies (Figure 2E) confirms statistical significance of HS-induced decrease in ADL84 staining and full recovery of the level of staining after recovery period in Kc cells. The same experiment in S2 cells also demonstrated significant decrease in ADL84 staining after HS (Figure 2E).

Immunofluorescence analyses using ADL84 monoclonal antibodies in Kc cells revealed the partial disappearance of the signal for nonphosphorylated (at S25) lamin Dm upon HS induction (Figure 2F). Since many posttranslational modifications other than phosphorylations (e.g., methylation, acetylation) or protein-protein interactions may theoretically affect the availability of this site to antibodies, we analyzed available databases for empirically detected modifications or presence of potential motifs for such modifications and interactions and we found none except mentioned above PIN1 and 14-3-3 protein zeta motifs. Nevertheless, the IF data from ADL84 staining were shown as additional demonstration of decrease of staining, but our calculations of lamin Dm conversions were based on quantification of Western blots only. Interestingly, data presented in Figure 2 demonstrate that the difference in cell origin and gene expression profile (also no lamin C expression) between Kc and S2 cells reflect their different response to HS and recovery at the protein level of Top2, Hsf and partly for total fraction of lamin Dm. Similarly, induction of increased level of S25 phosphorylation differs in the intensity of the effect between Kc and S2 cells as the changes of the total lamin Dm levels differ in Kc and S2 cells. Interestingly, Top2 protein relocation to nuclear lamina and "granular phenotype" of staining induced in heat shocked cells are identical in both cell lines (Figure 1A and 1B).

**Stress reversibly changes the distribution of Top2 and chromatin but does not affect the distribution of lamins.**

Since thermal stress induces the new *in vivo* binding sites for Top2 on chromatin and affects the composition of isolated karyoskeletal structures (nuclear matrix/chromosomal scaffold) isolated from heat shocked cells [66], [70], we investigated the distribution of the Top2 protein upon heat stress and recovery in Kc cells (Figure 3A) and embryos (Figure 3B and C); see also Figure 1A and B for Kc and S2 cells. Immunofluorescence analyses of Kc cells for Top2, Hsp70 and lamin Dm indicated the relocation of Top2 and/or modification of staining pattern upon HS induction from an intranuclear, mostly homogenous distribution to more lateral distribution with frequently observed spherical Top2 bodies and/or granules (Figure 3A arrows and Figure 1A and B arrows and arrowheads). Densitometry analyses confirmed the observed redistribution of Top2. Similar induced changes in distribution of Top2 staining were detected in early embryos (stage 10-12, Figure 3B) and embryo region with aenocytes as revealed by lamin C positive staining (Figure 3C). We did not detect any changes in lamin Dm staining or lamin C staining in Kc cells and embryos (Figure 3A, B and C). Please note that the redistribution of Top2 during HS was reversible both in Kc, S2 and embryonic cells.

The quantification of the immunofluorescence data for Top2 relocation in embryos (Figure 3D demonstrates magnification of typical staining, section of 3B) allowed for calculation of statistical significance of relocation of Top2 to the sublaminal region of cell nuclei (Figure 3E). To test whether the redistribution of Top2 is correlated with the redistribution of DNA, we chose third-instar larval nuclei, which are poliploidic and have clearly visible chromatin. Figure 3F shows the relocation of chromatin to nuclear periphery regions, which was statistically significant (Figure 3G).

Immunofluorescence analyses of localization of other nuclear antigens during HS and recovery in Kc cells indicated the expected relocation of Hsp90 protein from cytoplasmic location only into mixed cytoplasmic and nuclear location (Supplemental Figure 3A). Please note the lack of HSF and Hsp90 staining in nuclei regions with condensed chromatin. We did not detect visible changes in distribution of lamin Dm, HDAC1, LBR, bocksbeutel and RNA polymerase 2 pS5 in Kc cells (Supplemental Figure 3B, C and D). In embryos, HS induced decreased staining inside nuclei for HP1 protein and a small decrease in intranuclear signal for HSF protein (Supplemental Figure 4A and 4C, respectively). No visible changes were detected for Polymerase 2 pS5 and HDAC1 (Figure 4B and 4D respectively).

**Heat shock induction changes the solubility of lamin Dm, Top2, HDAC1 and HSF**.

Since we demonstrated that HS affects the level and distributions of Top2 and chromatin, we tested the solubility of lamin Dm, Top2 and other nuclear proteins in Kc and S2 cells (Figure 4A and 4B, respectively). We decided to use buffers with three concentrations of NaCl: 50 mM, 150 mM, and 500 mM NaCl. They were chosen as most frequently used to isolate fully soluble lamin fractions and soluble nuclear proteins (50 mM; low salt buffer), for nuclear proteins less soluble and fraction of “soluble” lamins (150 mM; medium salt buffer) and polymerized lamins and nuclear non-histone proteins

fraction (500 mM; high salt buffer). We compared the solubility of proteins from control cells and cells after HS. A comparison was made between normal conditions and heat shock induction within each fraction independently. Extracts were analysed upon SDS-PAGE electrophoresis and western blot staining with proper antibodies, followed by densitometry.

We observed significant alterations in the solubility of all analyzed proteins both in Kc cells and S2 cells although not in all fractions. In Kc cells, HS induced statistically significant increase of the fraction of lamin Dm in medium and high salt extracts, Top2 protein level from HS cells was decreased in low salt and increased in medium salt extracts. HDAC1 protein level in HS was also decreased in low salt and increased in high salt fraction. HSF protein level was increased in lysates, which was expected from its level in cell nuclei and increased translation during heat shock. There was also a decrease in HSF protein in low salt extracts and an increase in medium salt and high salt extracts. We also tested if there is any difference in extractability or level of lamin Dm1 and Dm2 forms using ADL84 antibodies. The low salt extracts from control cells demonstrated a much higher level in low salt fraction, which means that the higher level of lamin $Dm_1$ form (unphosphorylated at S25) was in low salt extract comparing to HS conditions. This indicates that fraction of lamin Dm ($Dm_2$) with phosphorylated S25 is less soluble at this condition, which in turn may indicate modified properties or interactions, or both.

In the same experiment with S2 cells we detected similar but not identical significant changes between extracts from normal and HS cells. Total lamin Dm fraction was increased in medium salt buffer (as in Kc cells) but decreased in low salt buffer (no difference in Kc cells). The Top2 fraction was increased only in low salt extract in S2 cells. HDAC1 level was decreased in low salt extract and increased in high salt extract. The HSF level was decreased in low salt and increased in medium salt and high salt buffer. No changes in extract fractions were detected for staining with ADL84 antibodies in S2 cells (not shown). The general trend detected in both cell lines for all proteins was the decrease of their levels in low salt fraction and increase in extracts with medium or/and high salt buffer (HSF, HDAC1, Top2, lamin Dm total, lamin Dm pS25). The only exceptions were lamin Dm in Kc cells (no decrease in low salt buffer, increased level in medium and high salt) and Top2 in S2 cells with decreased level only in low salt buffer (no changes in other fractions). Therefore, all analyzed proteins significantly changed their solubility in buffers, and the majority of the proteins have the same pattern or trend of changed solubility in both cell lines. Additionally, we confirmed previously shown data (Figure 2C and D) that heat shock induction, especially in S2 cells, induced a higher level of HSF, HDAC1 and Top2.

Supplemental Figure 5 demonstrates one of the many (at least 9) Western blots with a typical pattern of distribution of analyzed proteins between extracts from Kc and S2 cells for illustration of Western blots, lamin Dm forms ratios and quality of staining. Please note that in Kc cells there was clearly visible lower level of Top2 in low salt fraction from HS samples (Supplemental Figure 5A), higher level of HSF protein in HS lysate, lower level in low salt fraction and higher level in medium and high salt fractions.

For HDAC protein, a lower level was detected from HS cells and predominantly higher level of protein in a high salt buffer fraction. Please note that the total lamin Dm level is predominantly higher in the high salt buffer. Please note the modified ratio between the intensities of lamin $Dm_1$ and $Dm_2$ bands between control extracts and HS extracts.

When one looks at the lamin Dm fraction levels stained with ADL84 antibody (non-phosphorylated S25-specific) in extracts from control and HS Kc cells, the much lower signal was detected in low salt buffer comparing to normal extract (Supplemental Figure 5A). Similar analyses for S2 cell protein extracts from control and HS cells (Supplemental Figure 5B) demonstrated similar trends for HSF protein levels and HDAC1 protein levels (e.g. higher levels in medium salt buffer for HS extracts and higher levels in high salt extracts. Different ratios of lamin $Dm_1$ and $Dm_2$ were also detected between control and HS extracts, especially in fractions, but with lesser differences comparing to Kc cells (Supplementary Figure 5B; lamin Dm total).

**Lamin Dm interacts with topoisomerase II directly and through adjacent chromatin DNA regions, and interactions are increased during heat shock**

In earlier studies on Top2 and lamins, we confirmed that both proteins bind to chromatin and nucleic acids both *in vitro* and *in vivo* [58]. Here we tested whether these proteins interact with each other. Immunofluorescence analyses of the distribution of lamin Dm and Top2 revealed that the vast majority of the lamin Dm and Top2 proteins are located separately within typical cell nuclei. In polyploid nuclei of different poliploidity lamin Dm is located at the nuclear lamina and Top2 is more or less evenly dispersed within the nuclear interior, which is correct for cells in cell culture, in embryos and larvae (Figure 5A, upper left picture). Figure 5A, upper right and lower left demonstrates typical staining for lamin Dm and Top2 in polytenic nuclei of salivary glands, while lower right Panels demonstrate typical staining for lamin Dm and Top2 in diploid cells. Using the Proximity Ligation Assay (PLA) we demonstrated the colocalization (red signal) between Top2 protein and lamin Dm in Kc cells (Figure 5B, upper panels) and in polytenic salivary glands cell nuclei of the 3$^{rd}$ larval stage (Figure 5B, lower panels). Please note the lack of signal in single antibodies controls. In diploid cells we discovered typically several or more signals/loci (colocalization sites) for lamin Dm and Top2 interactions. In polytenic nuclei we detected many loci, also with different intensity and size. The 3D analysis of distribution of signal demonstrated that most loci were distributed at the chomosomes-nuclear lamina borders but a smaller fraction also inside cell nuclei (see Supplemental Movie 1 and Supplemental Movie 2 for 3D images). PLA assay performed on isolated imaginal discs (Figure 5C) from control larvae and larvae subjected to HS demonstrated the increase in number and size of colocalization loci in nuclei from HS induced larvae when compared with control larvae. Similar PLA tests with normal and heat shocked Kc cells (Figure 5H) also demonstrated the heat shock induced number of colocalization loci for lamin Dm and Top2. The increase in colocalization loci for lamin Dm and Top2 calculated by counting all foci and all nuclei

and their average ratio per nucleus was statistically significant (Figure 5I).

In order to confirm that lamin Dm and Top2 proteins colocalization in Kc cells and larvae, revealed in PLA assays, is the result of their interactions we performed immunoprecipitation from Kc cells native extracts (medium salt buffer) using affinity purified rabbit anti lamin Dm antibodies and affinity purified rabbit antibodies anti Top2 followed by western blot analyses (Figure 5D). Blots were probed with rabbit anti Top2 antibodies and monoclonal ADL67 antibodies for lamin Dm. The co-IP experiment result suggested the interaction of lamin Dm and Top2 in extracts under native conditions (medium salt buffer for extraction and IP procedure; Figure 5D). Results of the similar experiment with additional S7 nuclease treatment (on beads) and following additional washing steps demonstrate that the co-IP of the proteins under native conditions did not depend on their interaction with nucleic acids (Figure 5E).

Since only minor fraction of lamins can be extracted from Kc cells nuclei under medium salt buffer conditions while higher salt conditions may destroy their protein-protein interactions, we decided to use crosslinking conditions (PFA) before extraction under stronger conditions (150 mM NaCl, 1% Triton X-100, 0.1% SDS) and added additional sonication step in order to fragment chromatin DNA into about 500 bp fragments (see M&M section for details). This sonication step we adopted from, optimized by us, protocol for ChIP-seq for Top2 and lamin Dm experiments running in our lab since such conditions provided efficient lamin Dm and Top2 immunoprecipitation both for our IP and for ChIP-seq. For the experiment we used two populations of Kc cells: growing in normal conditions and with induced heat shock to see potential differences between normal conditions IP and HS conditions IP as one might expect from PLA experiments data.

Figure 5F demonstrates the typical result of such immunoprecipitation for lamin Dm and Top2 proteins using the same as above rabbit antibodies, while Figure 5G shows the magnified part of the Figure 5F demonstrating better the composition of lamin $Dm_1$ and $Dm_2$ fractions in extracts and IP outcome. As expected, extracts from normal and heat shocked Kc cells differed in lamin Dm forms composition and immunoprecipitation with lamin Dm antibodies and anti Top2 antibodies does not disturbed their composition (Figure 5F and 5G), compare input with both IPs and lamin staining. Interestingly, IP anti Top2 detected co-immunoprecipitated lamin Dm fractions retaining the same staining pattern as in the input and IP for lamin Dm (Figure 5F, co-IP Top2). This might suggest that detected lamin Dm-Top2 interaction is independent of lamin Dm S25 phosphorylation and potential N-terminal fragment conformation change. The demonstration that the lamin Dm and Top2 interaction was shown in both ways of IP makes this interaction more probable *in vivo*. The second conclusion from this experiment (Figure 5F) is that the stronger bands were detected for co-IP partners comparing normal conditions and heat shock. This suggested increased interaction between both proteins (or their protein complexes, or both) during heat shock and confirms the PLA data regarding increased contacts between them during heat shock.

To gain better insight into lamin Dm-Top2 interactions with chromatin, nucleic acids and themselves, we decided to use our previously used technique of *in vivo* BrdU labeling of DNA, *in vivo* photocrosslinking, immunoprecipitation and $^{32}P$ labeling of nucleic acids bound to proteins followed by WB and autoradiography/phosphoimager analyses [58], [59], see also M&M for the full procedure description.

The entire set of experiments with Kc cells fed with BrdU, UV crosslinking, cell lysis under denaturing conditions followed by sample preparation, immunoprecipitation, washing, radioactive labeling of crosslinked nucleic acids associated with immunoprecipitated (separately) lamin Dm and Top2, followed by labelling with radioactive gamma ATP and polynucleotide kinase (PNK) have been performed exactly as published earlier [58], [59]. The procedure itself is technically challenging and needs to be adjusted to many factors including efficiency of binding nucleic acids *in vivo* by the proteins of interests. This dependence is identical as with IP procedure for ChIP-seq experiments. Top2 protein, as enzyme processing DNA and also structural protein involved in DNA and RNA binding *in vivo* crosslinks to nucleic acids in the procedure quite easy and efficiently. Lamin Dm binds to nucleic acid with low efficiency and required long optimization procedures.

The method was initially developed for detection of DNA binding proteins in protein-DNA complexes. The method sensitivity depends on the efficiency of the particular protein to directly be in contact with nucleic acid similarly to chromatin immunoprecipitation step in ChIP-seq procedure thus the higher association of particular protein to nucleic acid the more efficient crosslinking. In order to make the method more efficient, the UV-sensitive, modifed, bromo-deoxyrybonucleotude (BrdU) was fed to cells to increase crosslinking efficiency. Additionally, Top2, as a dimeric enzyme acting on DNA *in vivo,* forms transiently a covalent complex with DNA through active center residue (in fly it is Y785) and one of the two DNA strands. This complex can be catched using denaturing lysis conditions and enhanced using some Top2 inhibitory drugs. Please see Discussion section for the longer discussion of this method and Top2 drugs. Figure 6A demonstrates typical western blot from such procedure when radioactive labeling step (on beads) was omitted (no $^{32}P$ gamma-ATP and PNK kinase added). Please note that the procedure outcome was load-sensitive and nuclease-sensitive from the point of IP of lamin Dm itself and from co-IP of Top2 level. As expected, blot demonstrates co-IP of Top2 with lamin Dm and sensitivity of UV-crosslinking procedure to additional nuclease treatment in efficiency of IP anti lamin Dm, measured by diminishing the co-IP Top2 levels beyond western blot detection (Figure 6A, load +S7 lines). This indicates that in this experimental procedure lamin Dm-Top2 co-IP was mostly dependent on nucleic acids bound by the proteins. We discussed this issue in depth in the Discussion section.

Figure 6B demonstrates the result of almost the same experiment as previous one but with complete, entire procedure of the *in vivo* BrdU labeling of DNA, UV-crosslinking, immunoprecipitation, $^{32}P$ (gamma ATP) and PNK kinase mediated labeling of nucleic acids, western blotting and autoradiography/phosphoimager analyses

performed on Kc cells (Figure 6B, WB - western blotting and $^{32}P$ – autoradiography). Please note that IP anti lamin Dm co-precipitates also Top2 protein and the amount of the co-precipitated Top2 protein, as well as the radioactive label associated with Top2 band were sensitive to additional nuclease treatment. The similar trend we detected for lamin Dm protein band and associated radioactive label (Figure 6B, WB and $^{32}P$: Top2 and Lam Dm). Similarly to the previous experiment with IP anti lamin Dm (Figure 6A), increasing amounts of nuclease decreased the co-immunoprecipitated Top2 band and associated radioactive label up to total disappearance of the Top2 band in Western blots and autoradiography. Higher levels of nuclease also decreased the level of lamin Dm in IP and totally diminished the associated label. This result was consistent with the previous experiment with lamin Dm immunoprecipitation (Figure 6A). Therefore, we suggest that our crosslinking, IP and radioactive labeling procedure detects the fraction of lamin Dm and Top2 associated with nucleic acids *in vivo* (see [58], [59]) and a fraction of the nucleic acid–associated proteins might reside on the same nucleic acid on the same or adjacent sequences.

We previously reported that lamin Dm and Top2 bind both DNA and RNA *in vivo* in Kc cells [58], [59]. In order to test if Top2 and lamin Dm change their properties of nucleic acid binding during heat shock induction we tested in control and heat shocked Kc cells the sensitivity of bound nucleic acid label by the proteins to DNase 1 and RNase A in our crosslinking, IP and labeling procedure (Figure 6C). No changes in the sensitivity of label between control and heat shock were detected but only increased general nucleic acid association with Top2 in heat shocked cells (Figure 6C, Normal-lanes 2-4; HS-lanes 5-7). Please see also Figure 6E for heat shock induced increased binding to nucleic acids by lamin Dm and Top2. The general increase in nucleic acid binding by both proteins during heat shock seems to be in agreement with increased interaction of both proteins with themselves demonstrated in PLA experiments (Figure 5C, H and I) and increased co-IP of both proteins in denaturing conditions (Figure 5F and G).

Based on the demonstrated earlier changes in solubility of tested proteins during heat shock, in next experiment we tested the lamin Dm and Top2 nucleic binding efficiency in soluble (150 mM NaCl in buffer) and insoluble (500 mM NaCl in buffer) fraction of Kc cells extract. Figure 6D demonstrates the IP and labeling experiment for lamin Dm and Top2 with Kc extracts. The highest nucleic acid binding efficiency was detected in the soluble fraction of lamin Dm and Top2 while the lowest was detected in insoluble fraction, also for both proteins. Please note the presence of Top2 radioactive band co-precipitated with soluble lamin Dm fraction, not detected by western bloting. The strongest and direct evidence of heat shock induced increased binding of Top2 and lamin Dm with nucleic acids in Kc cells is demonstrated in Figure 6E. Induction of heat shock results in increased association of both proteins with nucleic acids and after recovery time this nucleic acid association returns to normal, control conditions.

In order to test if there might be any preferences to the sequences being enriched preferentially upon heat shock induction we performed experiment on Kc cells with the presence of both BrdU and distamycin in cells, induced heat shock followed by the

entire procedure for UV-crosslinking, IP, labeling, western blotting and autoradiography. Previously, we reported that lamin Dm and Top2 bind *in vivo* both AT-rich and GC-rich DNA fragments using distamycin and chromomycin [58], [59]. Figure 6F indicates, as expected, that heat shock induced increased binding to nucleic acids for both proteins and distamycin decreased the radioactive label associated with lamin Dm. During heat shock distamycin also decreased the radioactive label on lamin Dm band comparing to control band. This suggests that lamin Dm associates with nucleic acids at the AT-rich sequences with similar proportion as in the control cells. Top2 protein band was associated with nucleic acid in both conditions in different ways. In control, we detected no or small effect of distamycin and a small decreasing effect during heat shock in radioactive label association. Which suggests that no dramatic changes in DNA/RNA binding properties or AT/GC rich sequence were detected. Figure 6G demonstrates the control experiment performed in Kc cells showing no induction of the expression of inducible Hsp70 protein by the experimental procedure used in this section.
Overall, based on the Figure 6 and previous experiments data we demonstrated, for the first time, that heat shock induction increased the level of S25 phosphorylation in lamin Dm which was associated with changes in the solubility of protein and increased association with nucleic acids *in vivo*.

We demonstrated that Top2 alters its distribution pattern and solubility during heat shock, and this altered Top2 distribution is also associated with chromatin relocation in larval polyploid cells. We demonstrated using PLA and two ways co-IP experiments that lamin Dm interacts with Top2, and heat shock increased the interaction between them. Proteins associations with nucleic acids increased upon heat shock induction, and some fractions of lamin Dm and Top2 bind the same or adjacent nucleic acid regions.

Please note that the observation on S25 phosphorylation reversible increase associated with heat shock is the first ever report, as well as the report on lamin Dm and Top2 interaction and the heat shock induced increased interaction associated with increased nucleic acid association.

## DISCUSSION

Lamin Dm, as the rest of B-type lamins, has been involved, together with A-type lamins and interacting proteins, in chromatin organization forming LADs domains at the nuclear lamina and nucleoli (nLADs) and at least is indirectly involved in formation of TADs [16], [83]–[87]. Interestingly, lamin Dm plays more important role in direct interactions with DNA and chromatin comparing to B-type lamins in vertebrates, since fly lamin C (A-type lamin) does not bind DNA *in vivo,* while vertebrate lamins A (but not vertebrate lamin C) do bind DNA *in vivo* and have farnezylation motif, removed upon assembly in nucleus. *Drosophila* lamin C does not have at all farnezylation motif, in this

is similar to vertebrate lamin C (a splicing variant of *LMNA* gene). Therefore, also in fly differentiating cells, when lamin C starts to be present, all DNA/chromatin direct interactions with nuclear envelope, through farnezylation motif/anchor, aimed at tethering the complexes, have to involve lamin Dm but not lamin C (see Zielinska et al 2025 for fly lamins major interactors). This might, at least in part, explain the differences in heat shock response between Kc cells and S2 cells or early embryos (e.g., shorter degradation time of Hsp70 during recovery in S2 and embryos, weak effect of S25 phosphorylation, stronger effects of Top2 and HSF level induction and protein solubility changes). The other reasons are global differences in gene expression profile between normal Kc and S2 cells and global differences in gene expression modulation during heat shock which altogether leads to different rearrangements of lamins and Top2 interactome [88]–[91]. Nevertheless, in differentiating cells of Metazoa (thus *Drosophila* as well), B- and A-type lamins form a hub or docking platform for integration of signaling pathways, including mechanosensing and mechanotransduction, between cell nucleus, cytoplasm and extracellular matrix [16], [17], [21], [92]. Therefore, we used a well-known fruit fly model system of Kc and S2 cells and, if necessary, fly tissues from early embryos to 3$^{rd}$ instar larvae. Both cell lines have been widely used for mapping *in vivo* Top2 binding sites under normal conditions and during heat shock by many laboratories, and there have been many reports on the mapping of several heat shock-induced Top2 binding sites [11], [20], [55], [70], [93].

To monitor heat shock effect induction, we selected an inducible form of the Hsp70 protein for WB and IF studies and a set of inducible heat shock protein-coding genes for RT–qPCR. We also observed the changed mobility of Hsf protein, which has been known to be phosphorylated during heat shock and changed mobility on Western blots [94]. We decided that Hsp70 protein would be the better choice for a marker of stress comparing with Hsf since its dephosphorylation takes place earlier, and much faster comparing to the restitution of transcriptome and proteome from changes induced by heat shock. We selected the HS induction time at 60 minutes to allow for efficient transcription and translation into a protein of the first round of heat shock-inducible genes [95]. Their protein products should have affected the chromatin structure at least at the heat shock factor-dependent genes and efficiently undertaken the transcription of secondary waves of heat shock-inducible genes with associated changes in chromatin structure and protein complexes associated with them. In Kc and S2 cells, we typically start to detect inducible Hsp70 protein *via* WB after 5-10 min of HS (not shown), but the transcripts can appear much earlier [95], [96]. The almost total disappearance of Hsp70 protein band during recovery (Figure 1C) at 24 hours in both cell lines is the result of protein degradation but not a dilution due to the cells proliferation, since doubling time for both cell lines is about 24-28 hours and in S2 cells at that time significant amount of Hsp70 protein already disappears while in embryos after 4h recovery time no Hsp70 were detected in IF staining (Supplementary Figure 1). The fact that in Kc cells after 6 hours of recovery time Hsp70 protein further increases may result from higher expression level and/or more stable transcripts for Hsp70, due to the different transcriptome pattern in control cells and during heat shock or due to the much more

complex transcriptome, proteome and more complex protein complexes and their rearrangement processes in Kc cells. We tested the viability of the cells during the experiment and recovery and found that the vast majority of the cells fully recovered from the HS, as indicated by Hsp70 WB and IF results.

Since the transcripts of typical reference housekeeping genes were not fully stable during HS and recovery, we selected a set of four reference transcripts for RT–qPCR studies (18S/28S RNA, actin 5C and tubulin 84B) instead of single reference gene (Supplementary Figure 2). Interestingly, the level of induction of selected HSP genes was lower in S2 cells than in Kc cells. This might reflect the differences based on different origin of cells and different gene expression profiles in general and/or specifically due to the expression of both lamins in Kc cells and only lamin Dm in S2 cells. Real-time PCR revealed no statistically significant changes in the transcript levels (those with changes less than 2x) of lamins, Top2, or Hsf. These findings are strongly correlated with the stable protein levels of lamins, Top2 and Hsf under normal conditions and during HS and recovery for Kc cells but not for proteins level in S2 cells (Figure 1D and Figure 2 A, B and C *versus* D). This again may reflect the differences in gene expression profile due to their different origin, the lack of lamin C and different response to stimuli due to the different organization of cell nucleus, chromatin and protein interactions in nuclei lacking lamin C (for current view of the nuclear lamina interactome and lamin interactome in *Drosophila* see [16], [29], [60], [61], [62]). WB analyses revealed reduced electrophoretic mobility of the Hsf protein under HS compared with that under normal conditions and recovery, which can be attributed to its phosphorylation upon HS. We also detected the increased conversion of lamin $Dm_1$ to the $Dm_2$ form (reduction of intensity of lower, faster migrating lamin band, and strengthening of the slower migrating (upper) band upon HS compared with normal conditions and recovery), which indicates that increased transient lamin phosphorylation, attributed to HS, significantly decreases upon recovery. Using unphosphorylated S25-specific monoclonal antibodies (recognizing protein unphosphorylated at S25), we demonstrated that this conversion is the result of at least one phosphorylation at site mapped to S25 in the N-terminal head domain. We demonstrated that the change in the level of S25 phosphorylation after heat shock was statistically significant in Kc cells and only marginally significant S2 cells (Figure2 C, D and E). Decreased fluorescence signal from ADL84 antibodies in immunofluorescent staining of Kc cells (unphosphorylated S25) during heat shock confirms the induced S25 phosphorylation detected on Western blots. We are aware of limitations of this method due to the potential epitope site masking by interactions and other posttranslational modifications. Therefore, we use available bioinformatic tools and databases for information on any discovered and potential sites in N-terminal lamin Dm modifications. No identified or potential methylation and acetylation sites have been found at this site except for phosphorylation, PIN1 and 14-3-3 zeta binding sites. Earlier studies with phosphatase treatment on Western blots revealed that ADL84 staining reappears after such treatment, which proves the phosphorylation sensitivity of ADL84 antibody and phosphorylation of extracted lamin Dm at S25. Nevertheless, all calculations were done

only on Western blots to be on a safe site for data interpretation.

We previously used an *in vitro* nuclear assembly system and transient transfection studies as well as a solubility assay and reported that a lamin Dm S25 phospho-mimicking (pseudophosphorylation) mutant presented a lower percentage of alpha-helical structures, lower polymerization properties, greater solubility and lower affinity for association with chromatin [23]. This finding suggests that *in vivo*, upon HS, such modified lamin Dm may participate in new interactions, possibly in different locations. Since fraction of mammalian interphase lamin A, when phosphorylated at the N-terminal Cdk1 ("mitotic") site, relocates to the nuclear interior from the nuclear lamina [97], [98] we may presume that S25 phosphorylation on lamin Dm may result also in relocation and modified interactions [97]; [99]; [100]. S25 in lamin Dm is not a Cdk1-specific site, but epitope mapping studies on lamin Dm point mutants have suggested that such modifications may affect the N-terminal lamin Dm structure up to the beginning of the alpha–helical rod domain and expose other, normally hidden phosphosites at N-terminus, including Cdk1 site (S45) or S50 (PKA site) [23], [29], [31]. Recent report on human lamin A phosphorylation on S22 (Cdk1 site) induced during heat shock and the mention that *Drosophila* lamin C fraction might also be phosphorylated on S37 (also Cdk1 site) during heat shock [98] suggest that HS-induced phosphorylation at N-terminus may be a conserved mechanism of response to heat shock or to induce a "different" fraction of lamin A when necessary for cells. In human, lamin A mitotic site (S22) is located in shorter head domain in 13 amino acid residues distance from alpha helical rod domain while fly lamin C mitotic site (S37) is 8 amino acid residues from alpha helical rod domain and is located deeper in protein with more limited access to kinase(s) active site comparing to lamin A. Nevertheless, in both proteins the access to the site is sterically limited to be accessed without prior reorganization of N-terminal structure of both lamins (by other sites phosphorylation?). In human lamin B and in fly lamin Dm (B-type) we have similar situation. Fly lamin Dm N-terminal region is longer and N-terminal mitotic site motif (S45) locates 8 aminoacid residues from the alpha helical rod domain while in both lamin B1 and B2 the spacing is 12 residues. In both situations there is also limited access to mitotic site by kinase(s) without rearranging the N-terminal region, likely by phosphatases and/or PIN 1 activity. Please note that in lamin A and C as well as lamin Dm and lamin B1/B2 there are phosphosites such as S25 in lamin Dm and PIN 1 (also 14-3-3 protein binding site) which may serve as reorganizations tools of N-terminal lamins domain [24], [29].

Our report on increased phosphorylation on S25 in lamin Dm (B-type lamin) may provide a hint about potential mechanism of opening of the N-terminal lamin domain for further modification and interactions both in normal physiological conditions as well as in heat shock or preparation for mitotic lamin disassembly. For a deeper discussion of the correlation between phosphorylation and lamin properties and potential interactions, see [24], [29].

Our IF studies indicated that upon HS, a fraction of Top2 relocates from more or less a homogenous, intranuclear distribution into a lateral, sublaminal distribution with frequently observed, many small granules or single, spherical Top2-dense granules,

and the relocation is reversible (Figure 1A and B, Figure 3A, B, C, D and E). Interestingly, in larvae nuclei, together with Top2 relocation, we also observed the relocation of chromatin to sub-laminal regions (Figure 3F and G).
Please also note the similar relocation pattern of Hsp90 protein, absent from center regions of nuclei, and similar distribution of HSF protein (Supplementary Figure 3A) during heat shock induction in Kc cells which is also reversible in recovery as well as the decrease in intensity of staining for HSF and its relocation into sublaminar regions during heat shock in early embryos and its transient effect (Supplementary Figure 4C). In early embryos we also detected a slight decrease in HP1 staining in heat shock which was also reversible during recovery (Supplementary Figure4A).

It was previously demonstrated that Top2 can exist in different fractions with distinct interactions [46], [49], solubility, phosphorylation, and activity [58]. Transient relocation of Top2 during heat shock, together with other essential for heat shock response proteins such as HSF and HP1 protein suggests more general relocation and interaction remodeling processes taking place in nucleus during heat shock than simple activation of heat shock response genes, shutdown of transcription of other non-essential genes or translation inhibition of non-heat shock related transcripts. These findings together with our data suggest that a relocated fraction of Top2 proteins may interact with different protein complexes in the nuclear lamina or its vicinity, and chromatin. This hypothesis might also be supported by lamins and Top2 interactome analyses (unpublished data, manuscript in preparation - see PhD thesis of Marta Rowinska [91]). An additional hypothesis might be that the fraction of the Top2 population may be associated with the formation of so-called stress granule complexes in the nucleus, since reports suggest the presence of stress granule protein markers inside mammalian cell nuclei [101], [102] but its presence in invertebrates has not been reported so far. The previously reported Top2 fraction associated with RNA particles may fit into both populations: new complexes on chromatin and RNA (transcripts, snRNAs and ribosomal RNA complexes temporarily bound; non-HS-associated transcripts and rybosomal precursors) and complexes that form nuclear precursors of cytoplasmic stress granules or creation of independent, nuclear stress granules/bodies [103]. Top2 relocation upon HS was also confirmed in embryos, which suggests that this is a common mechanism for Top2 relocation in response to HS. Notably, the detected relocations of proteins are fully reversible upon recovery.

Previous studies on lamins and Top2 in *Drosophila* demonstrated different fractions of Top2 and changes in solubility of lamin Dm, Top2 and other proteins (also RNA polymerase 2) resulted in higher level of aforementioned proteins in karyoskeletal fractions of cell nuclei isolated from heat shocked Kc, S2 cells and embryos [8], [23], [24], [26], [27], [55], [56], [58], [59], [103]–[106]. Such karyoskeletal structure has been named as an insoluble nuclear fraction or nuclear matrix. The latter is the older one, and its preparation may vary in many elements, but common denomination is the insolubility in high salt (NaCl) buffers.

Therefore, we performed an experiment on systematic detection of potential solubility changes in the most interesting nuclear proteins for us such as: lamins Top2, HSF, and HDAC1. Initial lysate was fractionated into the soluble fractions from low, medium and high salt extraction as the most frequent and typical conditions to extract nuclear proteins including lamins and Top2 proteins [58].

The lower salt concentration allows for the extraction of only fully "soluble proteins" from isolated or lysed cell nuclei, whereas 150 mM salt extracts most of the "soluble" proteins. High salt (500 mM NaCl) buffers have been typically used for the extraction of a major fraction of lamins both in mammalian and fly model systems of tissue-cultured cells [107]. We detected statistically significant changes in the level of proteins in extracts for all tested proteins in Kc and S2 cell lines. The differences were associated only with the question of which fractions were significantly affected. All proteins levels in both cell lines, except lamin Dm in Kc cells (no changes) were significantly decreased in heat shock in 50 mM NaCl fraction. All analysed proteins (except Top2; no changes) were at the significantly higher level in medium salt extracts or high salt extracts or in both extracts types during heat shock (Figure 4A and B). This suggests the general similar trend of modification of proteins themselves: e.g., lamin Dm phosphorylation on S25, HSF phosphorylation (Figure 2) and/or modification of interactions: e.g. HSF relocation (Figure 2C and D and Supplementary Figure 3A and 4C) and binding transcription complexes at heat shock responsive genes. This is also relocation (Figure 3) and modification of interaction, e.g., Top2 and lamin Dm increased colocalization and increased co-IP (Figure 5) and transient coordinated relocation of Top2 with chromatin in larval nuclei (Figure 5HI). For lamin Dm and Top2, the modification of solubility during heat shock was not only associated with increased interactions with themselves or their protein complexes, but also with increased association with chromatin (Figure 6).

BrdU labeling and *in vivo* UV crosslinking targets proteins in the vicinity (or bound) to DNA, the vast majority of the interactions detected in this method are DNA binding proteins and for this purpose the method has been developed. Therefore, most of the detected interactions should be sensitive to nucleic acid digestion. It also implies that any detected co-IP proteins might interact with the same or in proximity to the same sequence of DNA/RNA. Additionally, Top2 as dimeric enzyme acting on DNA binds DNA in chromatin catalytically as enzyme converting DNA topology and as chromatin structural protein and both functions may or may not take place next to lamin Dm associated chromatin. Lysis of Kc cells with SDS has been frequently used as a method to capture Top2 in the intermediate covalent complex between protein active center residue (in fly it is Y785) and one of the two DNA strands. This event has been used since early 80-ties to map *in vivo* DNA binding sites also induced by heat shock, also with Top2 drugs blocking the enzyme in covalent intermediate product with DNA [66], [70], [72], [108], [109], see also Top2 section of Introduction). Therefore, in our method nucleic acids associated with Top2 protein band may result from BrdU-mediated UV crosslinking and also from lysis of Kc cells with SDS, maintaining the covalent complex of Top2 Y785-DNA strand. Such catalytically generated Top2- strand of DNA complex

contributes to the total fraction of Top2-nucleic acids binding data. These “catalytically” generated sites have been found as heat shock induced sites. Our preliminary data from ChIP-seq experiments on Kc cells revealed that they are the minor fraction of detected DNA binding sites (unpublished data).

Immunoprecipitation with the use of the anti lamin Dm antibodies without radioactive labelling and autoradiography indicated that the efficiency of IP for lamin Dm (density of protein band) and co-immunoprecipitation efficiency of Top2 depends on the extent of S7 nuclease treatment in resin beads (Figure 6A). This suggests full dependence of Top2 co-IP on persistence of crosslinked nucleic acid fragments linking lamin Dm to Top2 (Figure 6A). Decrease of the lamin Dm band after additional S7 treatment may result either from association of additional lamin Dm proteins on the crosslinked nucleic acid strand but not immobilized to beads by interaction with IgGs or associated with removal of co-IP Top2-crosslinked to DNA strand also bound by lamin Dm protein. Similarly to previous experiment, the experiment with the use of the full IP procedure for immunoprecipitation of lamin Dm and nucleic acids radioactive showed that immunoprecipitated lamin Dm protein bands intensity depends on S7 nuclease treatment (Figure 6B). Increased S7 treatment on beads decreases the intensity of Top2 protein band co-immunoprecipitated with lamin Dm up to the total disappearance. This is also concomitant with a decrease in lamin Dm protein band intensity similarly to previous experiment. As expected, additional S7 nuclease treatment on beads decreases radioactive bands of Top2 and lamin Dm up to almost total disappearance. The remaining label suggests that autoradiography/phosphoimager detection is more sensitive comparing to western bloting (colorimetrical staining). During the procedure, large quantities of nucleic acid fragments did not crosslink to lamin Dm and Top2 protein bands contaminate/remain associated with beads and the samples and undergo radioactive labeling. As a result they are present in beads and consecutive washes eliminate them but not fully efficiently. Therefore, they may associate unspecifically to protein bands, especially with protein-rich bands - see IgG bands-associated radioactivity.

Figure 6C demonstrates the comparison of efficiency of binding to DNA or RNA by lamin Dm and Top2 in normal conditions (lanes 2-4) and during heat shock (lanes 5-7) respectively on autoradiography and western blot. After full anti lamin Dm and anti Top2 immunoprecipitation, additional digestion with DNase1 and RNase A on beads was performed. In general, heat shock increased the level of nucleic acid binding (- no treatment) but the sensitivity of the associated level for DNase 1 digestion and RNase A digestion was similar in normal and heat shocked Kc cells. This suggests that the mode/way of binding of both proteins does not change. Heat shock increased only the overall efficiency of nucleic acid binding, which might suggest an increased amount of the same complexes/interactions in heat shock. This combined with relocation of Top2 and modified solubility of all tested proteins suggests simple relocation of the same or similar complexes, with, for example Top2, from nuclear interior to the nuclear lamina.

The highest efficiency of *in vivo* associated nucleic acid was discovered for lamin Dm and Top2 in soluble fraction of proteins (Figure 6D). Please note the dramatic disproportion in lamin Dm protein association with nucleic acids comparing to Top2 protein nucleic acids association. In IP anti lamin Dm it is possible to detect radioactive Top2 band implying co–immunoprecipitated Top2 (no protein band visible on Western blots) demonstrating again co-IP of Top2 with lamin Dm and higher sensitivity of radioactivity detection comparing to Western blots visualisation. Similar experiments comparing the binding efficiency of lamin Dm and Top2 in normal Kc cells and heat shocked cells is shown in Figure 6E and clearly demonstrates the significant increase in nucleic acid labeling during heat shock for lamin Dm and Top2 protein.

Mammalian lamin B1 has been reported as binding to DNA *in vivo* through recognition of DNA sequence *via* minor groove in DNA using distamycin and chromomycin as a binders of minor and major groove in DNA respectively [110]. Therefore, we performed IP and labeling experiment using distamycin and using control Kc cells and heat shocked cells (Figure 6F). As expected, heat shock increased nucleic acid binding by lamin Dm and Top2 protein. Distamycin in Kc cells does not change the Top2 binding to nucleic acids in normal cells but decreases binding in heat shocked cells to the binding level of Top2 in control cells with and without distamycin. This might suggest that most of additional Top2 associations in heat shock are mediated through the minor groove of DNA. Lamin Dm–nucleic acid association decreased in normal cells and in heat shocked Kc cells fed with distamycin and the proportion of decrease suggests no changes in the mode of DNA binding by lamin Dm. None of the steps in the procedure used to identify nucleic acid associations with lamin Dm and Top2 in vivo induce stress or activate the heat shock response in the treated Kc cells. (Figure 6G). The overall conclusion from this set of experiments is that we confirmed our new discovery reported in this work about the interaction of lamin Dm with Top2 protein *in vivo*, confirmed that both proteins interact *in vivo* with nucleic acids and that both interactions increase during heat shock. We also demonstrated that lamin Dm and Top2 may reside on the adjacent sites on nucleic acids. This conclusion has been based on co-IP of both proteins, PLA colocalization data, and from *in vivo* crosslinking experiments.

Interestingly, despite of the different embryonic stages origin of Kc and S2 cells and associated gene expression profile and different, already programmed, differentiation direction, they demonstrated the same properties in respect to heat shock induced changes in solubility of tested proteins (Figure 4). This might suggest that heat shock response mechanisms are conserved and identical in both cell lines despite different transcriptome and proteome (e.g. lack of lamin C in S2 cells). Please note that this experiment also detected a statistically significant difference in the level of lamin Dm phosphorylated on S25 (pS25) (Figure 4 bottom diagram ADL84). The lack of statistical significant difference in the level of pS25 lamin in other fraction can be accounted for high deviations in experiment repetitions or low stability of the phosphate label in solutions, also in presence of standard phosphatase inhibitors cocktail or both events. This is the general problem for phosphosites identification and mapping when

longer times in solutions are necessary prior to LC MS/MS analyses [30].

Nevertheless, the decrease of lamin Dm pS25 fraction in low salt extract during heat shock, fully confirms our thesis of heat shock induced increase in S25 phosphorylation and suggests that this particular fraction does have different solubility/properties, interaction partners or all that features. Modified pS25 lamin Dm seems to have the same properties itself in respect to Top2 binding and heat shocked population of Top2 also has the same properties in binding (or the changes in binding preferences for both proteins are below detection) because the same proportions of lamin $Dm_1$ and $Dm_2$ in co-IP experiments with Top2 (Figure 5F and G) were detected. Nevertheless, the heat shock induced increase in PLA colocalization signal and the increased level of Top2 co-precipitated with lamin Dm and *vice versa* indicated that both proteins are during heat shock induced to get into proximity alone or with their own complexes. Detected relocation of Top2 closer to nuclear lamina area in Kc, S2 and embryonic cells (Figure 1 and Figure 3) induced by heat shock suggests relocation of Top2 as a probable mechanism. The detected correlation in larvae of relocation of Top2 and chromatin to nuclear lamina area (Figure 3F-G) might suggest that relocation of both Top2 (bound to chromatin?) and chromatin to the close proximity of nuclear lamina was involved. The latter hypothesis might be in favor of explaining increased association of lamin *Dm in vivo* with Top2 and also increased *in vivo* association of both proteins with nucleic acids (Figure 6). The co-precipitation of lamin Dm with Top2 and Top2 with lamin Dm under native conditions (Figure 5D) and its insensitivity to nuclease treatment suggest the elimination of potential intermediate nucleic acids as major contributor for mediation of the interaction (Figure 5E) and suggests that most of the lamin Dm interactions with Top2 are nucleic acid independent. The question whether the interaction detected under native conditions is mediated through associated other protein or proteins independently or at chromatin associated with nuclear lamina (e.g., LADs) remains to be tested. Experiments with PFA crosslinking prior to IP procedure demonstrate also the increased, in heat shock, co-IP of lamin Dm with Top2 and *vice versa* (Figure 5F and G). Preliminary data on interactome of both proteins based on above mentioned IP and LC MS/MS suggest rather complex interactomes and their dramatic changes induced by heat shock (Marta Rowinska PhD thesis, data in preparation).

Taking into the considerations all hypothesis based on our data on heat shock induced changes we propose a model of possible mechanisms explaining the experimental data and current view of the lamins and Top2 interactome (see Zielinska et al 2025 [29] for current fly lamin interactome network) involved in heat shock induced changes.

In normal conditions lamin Dm and small fraction of Top2 participate in multiprotein complexes associated with peripheral chromatin (cLADs and associated TADs) at the NL/NE/NPCs. Lamin Dm in normal conditions interacts with other NE and NL proteins (e.g., LEM-domain proteins, LINC complex, LBR), which help to organize chromatin complexes at the nuclear lamina and chromatin domains through interaction, mostly indirectly, with HP1, BAF and PcG)( for review see: [1], [2], [4], [29], [60], [89],

[111]–[113]). The equally important way of chromatin assembly into loops, TADs and LADs play Nuclear pore complexes, especially soluble nucleoporins (Nups) such as Nup107, Nup98, and Elys which together with other Nups link chromatin domains to NPCs and nuclear lamina Nup107-Nup160, NPCs, Elys, dLBR, HP1, Nup155, Nup53, Otefin, BAF, the LEM-domain and lamin Dm protein network. Lamin C, together with other nuclear proteins, takes part in these complexes making them more complicated, if these proteins are expressed in particular cell types in *Drosophila* [29].

Without lamin C presence (S2 cells, early embryogenesis), entire lamins' related complexes depend only on lamin Dm and this might partly explain differences in our experiments between Kc, S2 cells and embryos. Please note that lack of functional lamin C or presence of mutated lamin C with mutations resembling laminopathy, human lamin A mutations lead, in *Drosophila,* to muscular dystrophy phenotypes. Interestingly, one of the molecular background of muscle phenotype in muscles in induction of cellular stress [29], [114], [115]. Tethering of chromatin (cLADc, TADs, chromatin loops) to NPC/NL takes place through soluble Nups to insoluble Nups and core Nups of NPC complexes. Therefore, transcription intermediates, mRNPs complexes and other RNPs complexes (snRNPs, snoRNPs, splicing RNPs, ribosomal components) can be associated more or less transiently with chromatin complexes (LADs) on their way to or through NPCs.

After heat shock induction, some chromatin fibers, probably rich in genes being shut down during heat shock, may be relocated with their protein complexes (and associated Top2) to the vicinity of nuclear lamina (with lamin Dm) and NPCs creating, perhaps temporary, some sort of facultative LADs (fLADs) at the nuclear lamina tethered by lamin Dm and its interactome [1], [2], [4], [83], [113], [116]–[120]. This would explain increased colocalization and interaction of lamin Dm with Top2 protein (protein network?) and increased association of lamin Dm (and Top2) with nucleic acids/chromatin. Heat shock shuts down not only many genes but also inhibits translation of non-heat-shock related transcripts, which have been located in cytoplasm and in cell nucleus "in transit". Therefore, at the nucleus side they may be stored, together with their regulatory complexes, near the NPCs and nuclear lamina contributing to nucleic acids fraction associated with lamin Dm and Top2 as does chromatin and DNA relocated to nuclear lamina. Heat shock-induced increased phosphorylation at N-terminus may change the conformation of the N-terminal lamin Dm to be accessible for new interaction partners and possibly for further modifications to partly disassemble more lamin Dm proteins for new interactions to increase capacity to accommodate them into the complexes at the nuclear lamina. Relocation of Top2 to the nuclear lamina and demonstrated increased interaction of Top2 with lamin Dm together with Top2 protein localizing into nuclear speckles or multiple granules may also suggest the existence of "stress granules" containing Top2 and associated close to the nuclear lamina and NPCs.

## COMPETING INTERESTS

The authors declare that they have no competing interests.

## AUTHOR CONTRIBUTION STATEMENT

The authors confirm the contributions to the paper as follows: funding support, project administration (PI), concept of the study, general supervision and original draft writing: RR; work supervision, direct supervision and experiment planning: RR, MR, AT, JJ, MM, KP, AZ; conducting research, experimental work, data analysis and visualization: MR, AT, JJ, AZ, MM. Manuscript writing, editing and Figures preparation RR, MR, AT, JJ, AZ, MM. All the uthors reviewed the results and approved the final version of the manuscript.

## REFERENCES


[1] R. Berezney and D. S. Coffey, "Nuclear protein matrix: association with newly synthesized DNA.," *Science*, vol. 189, no. 4199, pp. 291–293, Jul. 1975.

[2] K. J. Pienta and D. S. Coffey, "A structural analysis of the role of the nuclear matrix and DNA loops in the organization of the nucleus and chromosome.," *J. Cell Sci. Suppl.*, vol. 1, pp. 123–135, 1984.

[3] T. Pederson, "Half a century of 'the nuclear matrix'.," *Mol. Biol. Cell*, vol. 11, no. 3, pp. 799–805, Mar. 2000.

[4] D. Small, B. Nelkin, and B. Vogelstein, "The association of transcribed genes with the nuclear matrix of Drosophila cells during heat shock.," *Nucleic Acids Res.*, vol. 13, no. 7, pp. 2413–2431, Apr. 1985.

[5] Y. B. Schwartz, E. S. Ioudinkova, S. A. Demakov, S. V Razin, and I. F. Zhimulev, "Interbands of Drosophila melanogaster polytene chromosomes contain matrix association regions.," *J. Cell. Biochem.*, vol. 72, no. 3, pp. 368–372, Mar. 1999.

[6] R. U. Pathak, A. Srinivasan, and R. K. Mishra, "Genome-wide mapping of matrix attachment regions in Drosophila melanogaster.," *BMC Genomics*, vol. 15, no. 1, p. 1022, Nov. 2014.

[7] G. I. Evan and D. C. Hancock, "Studies on the interaction of the human c-myc protein with cell nuclei: p62c-myc as a member of a discrete subset of nuclear proteins.," *Cell*, vol. 43, no. 1, pp. 253–61, 1985.

[8] P. A. Fisher, M. McConnell, A. Greenleaf, J. Lee, and D. E. Smith, "Heat shock-induced appearance of RNA polymerase II in karyoskeletal protein-enriched (nuclear 'matrix') fractions correlates with transcriptional shutdown in Drosophila melanogaster.," *J. Biol. Chem.*, vol. 264, no. 6, pp. 3464–9, 1989.

[9] M. McConnell, A. M. Whalen, D. E. Smith, and P. A. Fisher, "Heat shock-induced changes in the structural stability of proteinaceous karyoskeletal elements in vitro and morphological effects in situ.," *J. Cell Biol.*, vol. 105, no. 3, pp. 1087–98, 1987.

[10] W. C. Earnshaw and Heck, "Localization of topoisomerase II in mitotic chromosomes.," *J. Cell Biol.*, vol. 100, no. 5, pp. 1716–25, 1985.

[11] S. M. Gasser, J. F. Laroche, E. B. d. l. Tour, and U. K. Laemmli, "Metaphase chromosome structure. Involvement of topoisomerase II," *J. Mol. Biol.*, vol. 188, no. 4, pp. 613–29, 1986.

[12] W. C. Earnshaw, B. Halligan, C. A. Cooke, M. M. Heck, and L. F. Liu, "Topoisomerase II is a structural component of mitotic chromosome scaffolds.," *J. Cell Biol.*, vol. 100, no. 5, pp. 1706–15, 1985.

[13] R. Rzepecki, E. Markiewicz, and J. Szopa, "Identification of the proteins responsible for SAR DNA binding in nuclear matrix of Cucurbita pepo.," *Acta Biochim. Pol.*, vol. 42, no. 2, pp. 171–176, 1995.

[14] R. Rzepecki, E. Markiewicz, R. Adamiec, and J. Szopa, "Interaction of the Pisum sativum nuclear matrix proteins with SAR DNA.," *Acta Biochim. Pol.*, vol. 42, no. 1, pp. 75–81, 1995.

[15] T. Dechat, S. A. Adam, P. Taimen, T. Shimi, and R. D. Goldman, "Nuclear lamins.," *Cold*

*Spring Harb. Perspect. Biol.*, vol. 2, no. 11, pp. 1–22, 2010.
[16] X. Wong, A. J. Melendez-Perez, and K. L. Reddy, "The Nuclear Lamina.," *Cold Spring Harb. Perspect. Biol.*, vol. 14, no. 2, Feb. 2022.
[17] S. Osmanagic-Myers, T. Dechat, and R. Foisner, "Lamins at the crossroads of mechanosignaling," *Genes Dev.*, vol. 29, no. 3, pp. 225–237, 2015.
[18] S. R. Iyer, E. S. Folker, and R. M. Lovering, "The Nucleoskeleton: Crossroad of Mechanotransduction in Skeletal Muscle," *Front. Physiol.*, vol. 12, no. October, pp. 1–8, 2021.
[19] F. Donnaloja, F. Carnevali, E. Jacchetti, and M. T. Raimondi, "Lamin A/C Mechanotransduction in Laminopathies," *Cells*, vol. 9, no. 5, 2020.
[20] K. L. Wilson and R. Foisner, "Lamin-binding Proteins," *Cold Spring Harb. Perspect. Biol.*, vol. 2, no. 4, pp. 1–18, 2010.
[21] M. Dubinska-Magiera, M. Zaremba-Czogalla, and R. Rzepecki, "Muscle development, regeneration and laminopathies: How lamins or lamina-associated proteins can contribute to muscle development, regeneration and disease," *Cell. Mol. Life Sci.*, vol. 70, no. 15, pp. 2713–2741, 2013.
[22] R. Rzepecki and P. A. Fisher, "In vivo phosphorylation of Drosophila melanogaster nuclear lamins during both interphase and mitosis," *Cell. Mol. Biol. Lett.*, vol. 7, no. 3, pp. 859–876, 2002.
[23] M. Zaremba-Czogalla, K. Piekarowicz, K. Wachowicz, K. Kozioł, M. Dubińska-Magiera, and R. Rzepecki, "The different function of single phosphorylation sites of drosophila melanogaster lamin Dm and lamin C," *PLoS One*, vol. 7, no. 2, 2012.
[24] M. Machowska, K. Piekarowicz, and R. Rzepecki, "Regulation of lamin properties and functions: Does phosphorylation do it all?," *Open Biol.*, vol. 5, no. 11, 2015.
[25] F. Napoletano *et al.*, "The prolyl-isomerase PIN1 is essential for nuclear Lamin-B structure and function and protects heterochromatin under mechanical stress.," *Cell Rep.*, vol. 36, no. 11, p. 109694, Sep. 2021.
[26] M. Pałka *et al.*, "Laminopathies: what can humans learn from fruit flies," *Cell. Mol. Biol. Lett.*, vol. 23, no. 1, pp. 1–12, 2018.
[27] R. Rzepecki and Y. Gruenbaum, "Invertebrate models of lamin diseases," *Nucleus*, vol. 9, no. 1, pp. 227–234, 2018.
[28] D. Riemer, N. Stuurman, M. Berrios, C. Hunter, P. A. Fisher, and K. Weber, "Expression of Drosophila lamin C is developmentally regulated: analogies with vertebrate A-type lamins.," *J. Cell Sci.*, vol. 108 ( Pt 1, pp. 3189–3198, 1995.
[29] A. Zielińska, M. Rowińska, A. Tomczak, and R. Rzepecki, "Drosophila as a Model for Studying the Roles of Lamins in Normal Tissues and Laminopathies.," *Cells*, vol. 14, no. 17, Aug. 2025.
[30] M. Zaremba-Czogalla *et al.*, "Identification of new in vivo phosphosites on lamin Dm-the evidence of heterogeneity of phosphorylation sites in different Drosophila tissues," *Nucleus*, vol. 2, no. 5, 2011.
[31] U. Schneider, T. Mini, P. Jenö, P. A. Fisher, and N. Stuurman, "Phosphorylation of the major Drosophila lamin in vivo: Site identification during both M-phase (Meiosis) and interphase by electrospray ionization tandem mass spectrometry," *Biochemistry*, vol. 38,

no. 14, pp. 4620–4632, 1999.
[32] Y. Gruenbaum *et al.*, "Drosophila nuclear lamin precursor Dm0 is translated from either of two developmentally regulated mRNA species apparently encoded by a single gene," *J. Cell Biol.*, vol. 106, no. 3, pp. 585–596, 1988.
[33] D. E. Smith, Y. Gruenbaum, M. Berrios, and P. A. Fisher, "Biosynthesis and Interconversion of Drosophila Nuclear Lamin Isoforms during Normal Growth and in Response to Heat Shock," *J. Cell Biol.*, vol. 105, no. 2, pp. 771–790, 1987.
[34] N. Stuurman, N. Maus, and P. A. Fisher, "Interphase phosphorylation of the Drosophila nuclear lamin: Site-mapping using a monoclonal antibody," *J. Cell Sci.*, vol. 108, no. 9, pp. 3137–3144, 1995.
[35] J. M. Berger and J. C. Wang, "Recent developments in DNA topoisomerase II structure and mechanism," *Curr. Opin. Stuctural Biol.*, vol. 6, no. 1, pp. 84–90, 1996.
[36] J. Roca, J. M. Berger, S. C. Harrison, and J. C. Wang, "DNA transport by a type II topoisomerase: direct evidence for a two-gate mechanism," *Proc. Natl. Acad. Sci. U. S. A.*, vol. 93, no. 9, pp. 4057–62, 1996.
[37] J. Roca and J. . Wang, "DNA transport by a type II DNA topoisomerase: evidence in favor of a two-gate mechanism.," *Cell*, vol. 77, no. 4, pp. 609–16, 1994.
[38] E. M. Hildebrand *et al.*, "Mitotic chromosomes are self-entangled and disentangle through a topoisomerase-II-dependent two-stage exit from mitosis.," *Mol. Cell*, vol. 84, no. 8, pp. 1422-1441.e14, Apr. 2024.
[39] P. Buchenau, H. Saumweber, and D. J. Arndt-Jovin, "Consequences of topoisomerase II inhibition in early embryogenesis of Drosophila revealed by in vivo confocal laser scanning microscopy.," *J. Cell Sci.*, vol. 104 ( Pt 4, pp. 1175–85, 1993.
[40] S. DiNardo, R. Voelkel, and R. Sternglanz, "DNA topoisomerase II mutant of Saccharomyces cerevisiae: topoisomerase II is required for segregation of daughter molecules at the termination of DNA replication," *Proc. Natl. Acad. Sci. U. S. A.*, vol. 81, no. 9, pp. 2616–20, 1984.
[41] C. Holm, T. Goto, J. C. Wang, and D. Botstein, "DNA topoisomerase II is required at the time of mitosis in yeast.," *Cell*, vol. 41, no. 2, pp. 553–63, 1985.
[42] M. Iwai, A. Hara, T. Andoh, and R. Ishida, "ICRF-193, a catalytic inhibitor of DNA topoisomerase II, delays the cell cycle progression from metaphase, but not from anaphase to the G1 phase in mammalian cells," *FEBS Lett.*, vol. 406, no. 3, pp. 267–70, 1997.
[43] J. B. Rattner, M. J. Hendzel, C. S. Furbee, M. T. Muller, and D. P. Bazett-Jones, "Topoisomerase II alpha is associated with the mammalian centromere in a cell cycle- and species-specific manner and is required for proper centromere/kinetochore structure," *J. Cell Biol.*, vol. 134, no. 5, pp. 1097–107, 1996.
[44] C. E. Shamu and A. W. Murray, "Sister chromatid separation in frog egg extracts requires DNA topoisomerase II activity during anaphase.," *J. Cell Biol.*, vol. 117, no. 5, pp. 921–34, 1992.
[45] T. Uemura, H. Ohkura, Y. Adachi, K. Morino, K. Shiozaki, and M. Yanagida, "DNA topoisomerase II is required for condensation and separation of mitotic chromosomes in S. pombe," *Cell*, vol. 50, no. 6, pp. 917–25, 1987.
[46] Y. Adachi, M. Luke, and U. K. Laemmli, "Chromosome assembly in vitro: topoisomerase

II is required for condensation.," *Cell*, vol. 64, no. 1, pp. 137–48, 1991.
[47] W. I. Garinther and M. C. Schultz, "Topoisomerase function during replication-independent chromatin assembly in yeast.," *Mol. Cell. Biol.*, vol. 17, no. 7, pp. 3520–3526, Jul. 1997.
[48] E. R. Wood and W. C. Earnshaw, "Mitotic chromatin condensation in vitro using somatic cell extracts and nuclei with variable levels of endogenous topoisomerase II.," *J. Cell Biol.*, vol. 111, no. 6 Pt 2, pp. 2839–2850, Dec. 1990.
[49] F. Klein, T. Laroche, M. E. Cardenas, J. F. Hofmann, D. Schweizer, and S. M. Gasser, "Localization of RAP1 and topoisomerase II in nuclei and meiotic chromosomes of yeast.," *J. Cell Biol.*, vol. 117, no. 5, pp. 935–948, Jun. 1992.
[50] P. B. Moens and W. C. Earnshaw, "Anti-topoisomerase II recognizes meiotic chromosome cores.," *Chromosoma*, vol. 98, no. 5, pp. 317–322, Nov. 1989.
[51] D. Rose, W. Thomas, and C. Holm, "Segregation of recombined chromosomes in meiosis I requires DNA topoisomerase II.," *Cell*, vol. 60, no. 6, pp. 1009–1017, Mar. 1990.
[52] D. Rose and C. Holm, "Meiosis-specific arrest revealed in DNA topoisomerase II mutants.," *Mol. Cell. Biol.*, vol. 13, no. 6, pp. 3445–3455, Jun. 1993.
[53] M. Berrios, N. Osheroff, and P. A. Fisher, "In situ localization of DNA topoisomerase II, a major polypeptide component of the Drosophila nuclear matrix fraction.," *Proc. Natl. Acad. Sci. U. S. A.*, vol. 82, no. 12, pp. 4142–4146, Jun. 1985.
[54] P. A. Fisher, "Chromosomes and chromatin structure: the extrachromosomal karyoskeleton.," *Curr. Opin. Cell Biol.*, vol. 1, no. 3, pp. 447–453, Jun. 1989.
[55] V. H. Meller, P. A. Fisher, and M. Berrios, "Intranuclear distribution of DNA topoisomerase II and chromatin.," *Chromosom. Res. an Int. J. Mol. Supramol. Evol. Asp. Chromosom. Biol.*, vol. 3, no. 4, pp. 255–260, Jun. 1995.
[56] A. M. Whalen, M. McConnell, and P. A. Fisher, "Developmental regulation of Drosophila DNA topoisomerase II.," *J. Cell Biol.*, vol. 112, no. 2, pp. 203–213, Jan. 1991.
[57] F. Girard, B. Bello, U. K.laemmli, and W. J.gehring, "In vivo analysis of scaffold-associated regions in Drosophila: A synthetic high-affinity SAR binding protein suppresses position effect variegation," *EMBO J.*, vol. 17, no. 7, pp. 2079–2085, 1998.
[58] R. Rzepecki and P. a Fisher, "During both interphase and mitosis, DNA topoisomerase II interacts with DNA as well as RNA through the protein's C-terminal domain.," *J. Cell Sci.*, vol. 113, pp. 1635–1647, 2000.
[59] R. Rzepecki, S. S. Bogachev, E. Kokoza, N. Stuurman, and P. A. Fisher, "In vivo association of lamins with nucleic acids in Drosophila melanogaster," vol. 129, pp. 121–129, 1998.
[60] S. M. Gasser and U. K. Laemmli, "Cohabitation of scaffold binding regions with upstream/enhancer elements of three developmentally regulated genes of D. melanogaster.," *Cell*, vol. 46, no. 4, pp. 521–530, Aug. 1986.
[61] A. Bihani, A. K. Avvaru, and R. K. Mishra, "Biochemical Deconstruction and Reconstruction of Nuclear Matrix Reveals the Layers of Nuclear Organization.," *Mol. Cell. Proteomics*, vol. 22, no. 12, p. 100671, Dec. 2023.
[62] S. Kallappagoudar, P. Varma, R. U. Pathak, R. Senthilkumar, and R. K. Mishra, "Nuclear matrix proteome analysis of Drosophila melanogaster.," *Mol. Cell. Proteomics*, vol. 9, no.

9, pp. 2005–2018, Sep. 2010.
[63] R. Sureka, R. Wadhwa, S. S. Thakur, R. U. Pathak, and R. K. Mishra, "Comparison of Nuclear Matrix and Mitotic Chromosome Scaffold Proteins in Drosophila S2 Cells-Transmission of Hallmarks of Nuclear Organization Through Mitosis.," *Mol. Cell. Proteomics*, vol. 17, no. 10, pp. 1965–1978, Oct. 2018.
[64] I. Liebich, J. Bode, I. Reuter, and E. Wingender, "Evaluation of sequence motifs found in scaffold/matrix-attached regions (S/MARs).," *Nucleic Acids Res.*, vol. 30, no. 15, pp. 3433–3442, Aug. 2002.
[65] D. E. Smith and P. A. Fisher, "Identification, developmental regulation, and response to heat shock of two antigenically related forms of a major nuclear envelope protein in Drosophila embryos: application of an improved method for affinity purification of antibodies using polypeptide," *J. Cell Biol.*, vol. 99, no. 1 Pt 1, pp. 20–28, Jul. 1984.
[66] T. C. Rowe, J. C. Wang, and L. F. Liu, "In vivo localization of DNA topoisomerase II cleavage sites on Drosophila heat shock chromatin," *Mol. Cell. Biol.*, vol. 6, no. 4, pp. 985–992, 1986.
[67] R. D. Moir *et al.*, "Review: The dynamics of the nuclear lamins during the cell cycle - Relationship between structure and function," *J. Struct. Biol.*, vol. 129, no. 2–3, pp. 324–334, 2000.
[68] J. Lammerding, "Mechanics of the nucleus," *Compr. Physiol.*, vol. 1, no. 2, pp. 783–807, 2011.
[69] Y. Y. Shevelyov and S. V. Ulianov, "The Nuclear Lamina as an Organizer of Chromosome Architecture," *Cells*, vol. 8, no. 2, p. 136, 2019.
[70] A. Udvardy and P. Schedl, "The dynamics of chromatin condensation: redistribution of topoisomerase II in the 87A7 heat shock locus during induction and recovery," *Mol. Cell. Biol.*, vol. 13, no. 12, pp. 7522–7530, 1993.
[71] Y. Adachi, E. Käs, and U. K. Laemmli, "Preferential, cooperative binding of DNA topoisomerase II to scaffold-associated regions.," *EMBO J.*, vol. 8, no. 13, pp. 3997–4006, Dec. 1989.
[72] M. E. Borgnetto, S. Tinelli, L. Carminati, and G. Capranico, "Genomic sites of topoisomerase II activity determined by comparing DNA breakage enhanced by three distinct poisons.," *J. Mol. Biol.*, vol. 285, no. 2, pp. 545–554, Jan. 1999.
[73] A. O. Sperry, V. C. Blasquez, and W. T. Garrard, "Dysfunction of chromosomal loop attachment sites: illegitimate recombination linked to matrix association regions and topoisomerase II.," *Proc. Natl. Acad. Sci. U. S. A.*, vol. 86, no. 14, pp. 5497–5501, Jul. 1989.
[74] M. J. Guertin, K. L. Petesch, I. M. Zobeck, and J. T. Lis, "Drosophila Heat Shock System as a General Model to Investigate Transcriptional Regulation," *Cold Spring Harb. Symp. Quant. Biol.*, vol. 75, pp. 1–9, 2017.
[75] D. Klonaros, J. M. Dresch, and R. A. Drewell, "Transcriptome profile in Drosophila Kc and S2 embryonic cell lines," *G3 Genes, Genomes, Genet.*, vol. 13, no. 5, pp. 1–11, 2023.
[76] N. Wagner, D. Weber, S. Seitz, and G. Krohne, "The lamin B receptor of Drosophila melanogaster," *J. Cell Sci.*, vol. 117, pp. 2015–2028, 2015.
[77] U. K. Laemmli, "Cleavage of structural proteins during the assembly of the head of

bacteriophage T4.," *Nature*, vol. 227, no. 5259, pp. 680–685, Aug. 1970.
[78] E. Harlow and D. Lane, "Storing and purifying antibodies.," *Cold Spring Harb. Protoc.*, vol. 1988, pp. 283–318.
[79] R. Rzepecki and P. A. Fisher, "The study of Drosophila melanogaster lamin Dm phosphorylation in tissue culture Kc cells in vivo," *Cell. Mol. Biol. Lett.*, vol. 05, no. 2, p. 263, 2000.
[80] L. R. Alagar Boopathy, S. Jacob-Tomas, C. Alecki, and M. Vera, "Mechanisms tailoring the expression of heat shock proteins to proteostasis challenges," *J. Biol. Chem.*, vol. 298, no. 5, p. 101796, 2022.
[81] S. S. Teves and S. Henikoff, "The heat shock response: A case study of chromatin dynamics in gene regulation," *Biochem. Cell Biol.*, vol. 91, no. 1, pp. 42–48, 2013.
[82] M. Fritsch and C. Wu, "Phosphorylation of Drosophila heat shock transcription factor," *Cell Stress and Chaperones*, vol. 4, no. 2. pp. 102–117, 1999.
[83] P. R. Cook and D. Marenduzzo, "Transcription-driven genome organization: a model for chromosome structure and the regulation of gene expression tested through simulations.," *Nucleic Acids Res.*, vol. 46, no. 19, pp. 9895–9906, Nov. 2018.
[84] T. Sexton *et al.*, "Three-dimensional folding and functional organization principles of the Drosophila genome.," *Cell*, vol. 148, no. 3, pp. 458–472, Feb. 2012.
[85] S. V Ulianov *et al.*, "Order and stochasticity in the folding of individual Drosophila genomes.," *Nat. Commun.*, vol. 12, no. 1, p. 41, Jan. 2021.
[86] W. A. Bickmore and B. van Steensel, "Genome architecture: domain organization of interphase chromosomes.," *Cell*, vol. 152, no. 6, pp. 1270–1284, Mar. 2013.
[87] A. V Pindyurin *et al.*, "The large fraction of heterochromatin in Drosophila neurons is bound by both B-type lamin and HP1a.," *Epigenetics Chromatin*, vol. 11, no. 1, p. 65, Nov. 2018.
[88] L. Serebreni and A. Stark, "Insights into gene regulation: From regulatory genomic elements to DNA-protein and protein-protein interactions.," *Curr. Opin. Cell Biol.*, vol. 70, pp. 58–66, Jun. 2021.
[89] Y. Liao, X. Zhang, M. Chakraborty, and J. J. Emerson, "Topologically associating domains and their role in the evolution of genome structure and function in Drosophila.," *Genome Res.*, vol. 31, no. 3, pp. 397–410, Mar. 2021.
[90] E. Nazer, "To be or not be (in the LAD): emerging roles of lamin proteins in transcriptional regulation.," *Biochem. Soc. Trans.*, vol. 50, no. 2, pp. 1035–1044, Apr. 2022.
[91] M. Rowińska, "Identification of protein artners of lamin Dm and topoisomerase II under heat shock conditions in Drosophila melanogaster model system," 2024. [Online]. Available: https://bip.uni.wroc.pl/3543/postepowanie-w-sprawie-nadania-stopnia-doktora-w-dziedzinie-nauk-scislych-i-przyrodniczych-w-dyscyplinie-nauki-biologiczne-mgr-marta-rowinska.html.
[92] G. Ma *et al.*, "The nuclear matrix stabilizes primed-specific genes in human pluripotent stem cells.," *Nat. Cell Biol.*, vol. 27, no. 2, pp. 232–245, Feb. 2025.
[93] E. Kas, L. Poljak, Y. Adachi, and U. K. Laemmli, "A model for chromatin opening: Stimulation of topoisomerase II and restriction enzyme cleavage of chromatin by

distamycin," *EMBO J.*, vol. 12, no. 1, pp. 115–126, 1993.
[94] M. K. Singh *et al.*, "Heat Shock Response and Heat Shock Proteins: Current Understanding and Future Opportunities in Human Diseases.," *Int. J. Mol. Sci.*, vol. 25, no. 8, Apr. 2024.
[95] R. Ietswaart *et al.*, "Genome-wide quantification of RNA flow across subcellular compartments reveals determinants of the mammalian transcript life cycle.," *Mol. Cell*, vol. 84, no. 14, pp. 2765-2784.e16, Jul. 2024.
[96] R. Ben-Yishay and Y. Shav-Tal, "The dynamic lifecycle of mRNA in the nucleus.," *Curr. Opin. Cell Biol.*, vol. 58, pp. 69–75, Jun. 2019.
[97] V. Kochin *et al.*, "Interphase phosphorylation of lamin A," *J. Cell Sci.*, vol. 127, no. 12, pp. 2683–2696, 2014.
[98] L. Virtanen *et al.*, "Lamin A/C phosphorylation at serine 22 is a conserved heat shock response to regulate nuclear adaptation during stress," *J. Cell Sci.*, vol. 136, no. 4, 2023.
[99] N. Naetar *et al.*, "LAP2alpha maintains a mobile and low assembly state of A-type lamins in the nuclear interior.," *Elife*, vol. 10, Feb. 2021.
[100] J.-T. Chen *et al.*, "Identification of the lamin A/C phosphoepitope recognized by the antibody P-STM in mitotic HeLa S3 cells.," *BMC Biochem.*, vol. 14, p. 18, Jul. 2013.
[101] A. Sandqvist and L. Sistonen, "Nuclear stress granules: The awakening of a sleeping beauty?," *J. Cell Biol.*, vol. 164, no. 1, pp. 15–17, 2004.
[102] G. Biamonti and C. Vourc'h, "Nuclear stress bodies.," *Cold Spring Harb. Perspect. Biol.*, vol. 2, no. 6, pp. 1–13, 2010.
[103] V. H. Meller and P. A. Fisher, "Nuclear distribution of Drosophila DNA topoisomerase II is sensitive to both RNase and DNase.," *J. Cell Sci.*, vol. 108 ( Pt 4, pp. 1651–1657, Apr. 1995.
[104] P. A. Fisher and G. Blobel, "Preparation of a nuclear matrix--pore complex--lamina fraction from embryos of Drosophila melanogaster.," *Methods Enzymol.*, vol. 96, pp. 589–596, 1983.
[105] D. E. Smith, Y. Gruenbaum, M. Berrios, and P. A. Fisher, "Biosynthesis and interconversion of Drosophila nuclear lamin isoforms during normal growth and in response to heat shock," *J. Cell Biol.*, vol. 105, no. 2, pp. 771–790, 1987.
[106] P. A. Fisher, M. Berrios, and G. Blobel, "Isolation and characterization of a proteinaceous subnuclear fraction composed of nuclear matrix, peripheral lamina, and nuclear pore complexes from embryos of Drosophila melanogaster.," *J. Cell Biol.*, vol. 92, no. 3, pp. 674–686, Mar. 1982.
[107] V. Pekovic *et al.*, "Nucleoplasmic LAP2alpha-lamin A complexes are required to maintain a proliferative state in human fibroblasts.," *J. Cell Biol.*, vol. 176, no. 2, pp. 163–172, Jan. 2007.
[108] T. Andoh and R. Ishida, "Catalytic inhibitors of DNA topoisomerase II.," *Biochim. Biophys. Acta*, vol. 1400, no. 1–3, pp. 155–171, Oct. 1998.
[109] P. D. Varga-Weisz, M. Wilm, E. Bonte, K. Dumas, M. Mann, and P. B. Becker, "Chromatin-remodelling factor CHRAC contains the ATPases ISWI and topoisomerase II.," *Nature*, vol. 388, no. 6642, pp. 598–602, Aug. 1997.
[110] M. E. Ludérus, J. L. den Blaauwen, O. J. de Smit, D. A. Compton, and R. van Driel,

"Binding of matrix attachment regions to lamin polymers involves single-stranded regions and the minor groove.," *Mol. Cell. Biol.*, vol. 14, no. 9, pp. 6297–6305, Sep. 1994.
[111] N. Naetar, S. Ferraioli, and R. Foisner, "Lamins in the nuclear interior - Life outside the lamina," *J. Cell Sci.*, vol. 130, no. 13, pp. 2087–2096, 2017.
[112] J. Krefting, M. A. Andrade-Navarro, and J. Ibn-Salem, "Evolutionary stability of topologically associating domains is associated with conserved gene regulation.," *BMC Biol.*, vol. 16, no. 1, p. 87, Aug. 2018.
[113] S. V Razin, I. V Zhegalova, and O. L. Kantidze, "Domain Model of Eukaryotic Genome Organization: From DNA Loops Fixed on the Nuclear Matrix to TADs.," *Biochemistry. (Mosc).*, vol. 87, no. 7, pp. 667–680, Jul. 2022.
[114] S. G. Walker, C. J. Langland, J. Viles, L. A. Hecker, and L. L. Wallrath, "Drosophila Models Reveal Properties of Mutant Lamins That Give Rise to Distinct Diseases.," *Cells*, vol. 12, no. 8, Apr. 2023.
[115] G. S. Coombs *et al.*, "Modulation of muscle redox and protein aggregation rescues lethality caused by mutant lamins.," *Redox Biol.*, vol. 48, p. 102196, Dec. 2021.
[116] R. Cuesta, G. Laroia, and R. J. Schneider, "Chaperone Hsp27 inhibits translation during heat shock by binding eIF4G and facilitating dissociation of cap-initiation complexes," *Genes Dev.*, vol. 14, no. 12, pp. 1460–1470, 2000.
[117] D. A. Mir, Z. Ma, J. Horrocks, and A. Rogers, "Stress-Induced Eukaryotic Translational Regulatory Mechanisms.," *J. Clin. Med. Sci.*, vol. 8, no. 2, 2024.
[118] K.-H. Yeom *et al.*, "Tracking pre-mRNA maturation across subcellular compartments identifies developmental gene regulation through intron retention and nuclear anchoring.," *Genome Res.*, vol. 31, no. 6, pp. 1106–1119, Jun. 2021.
[119] R. Ben-Yishay, A. J. Ashkenazy, and Y. Shav-Tal, "Dynamic Encounters of Genes and Transcripts with the Nuclear Pore.," *Trends Genet.*, vol. 32, no. 7, pp. 419–431, Jul. 2016.
[120] D. A. Jackson and P. R. Cook, "Transcription occurs at a nucleoskeleton.," *EMBO J.*, vol. 4, no. 4, pp. 919–925, Apr. 1985.

## FIGURE LEGENDS

**Figure 1**

**<u>The analysis of expression of heat-inducible Hsp70 is an indicator of the efficiency of stress response and recovery</u>**

(A) Immunofluorescence staining of Hsp70 protein in Kc cells under normal (N), heat shock (HS, 1 h at 37 °C), and recovery (R) conditions. Recovery duration was 72 h. Fluorescence channels: blue – DAPI (nuclei), green – Top2, red – Hsp70, gray – lamin Dm, and merge. Arrows point to cell nuclei with typical Top2 multi-granular phenotype. Arrowheads point to cell nuclei with Top2 phenotype of single or few larger granules.
(B) Immunofluorescence staining of Hsp70 in S2 cells under normal (N), heat shock (HS, 1 h at 37 °C), and recovery (R) conditions. Recovery duration was 48 h. Fluorescence channels: blue – DAPI (nuclei), green – Top2, red – Hsp70, gray – lamin Dm, and merge. Arrows and arrowheads as in A.
(C) Western blot analysis of Hsp70 protein levels in Kc and S2 cells under heat shock and recovery conditions. The efficiency of recovery was assessed by monitoring the disappearance of the Hsp70 band over time. In addition to Hsp70, HSF was used as a stress response marker, and α-tubulin (α-Tub) served as a loading control. Protein levels were verified at multiple time points following 1 h of heat shock and during recovery at 6, 24, 48, 72, and 96 h. Normal (N) conditions were used as a reference for complete recovery.
(D) RT-qPCR analysis of the relative expression levels of selected transcripts involved in the heat shock response, including heat shock proteins (Hsp22, Hsp68, Hsp70, and Hsp83) and the transcriptional regulator Hsf, in Kc cells at different heat shock time points (15, 30, and 60 min). Fold changes were calculated using the ΔΔCt method, with normalization to control cells (N) and the endogenous reference gene Tub84B. Data represent the mean ± standard deviation from two biologically independent experiments, each performed with three technical replicates, except for two cases where only two technical replicates were available due to experimental limitations. qPCR reactions were performed using the QuantStudio™ 5 thermocycler, and data were analyzed using the Applied Biosystems™ qPCR analysis module, with additional calculations performed in Microsoft Excel. Final graphs were generated using GraphPad Prism 10.6.1.

**Figure 2.**

**Effects of heat stress on gene and protein expression, and phosphorylation status of lamin Dm, in *Drosophila* cell lines.**

**(A)** Relative mRNA expression levels of *LamDm*, *LamC*, *Top2*, and *Hsf* genes in Kc (black bars) and S2 (gray bars) cells following 1 hour of heat shock (HS) induction at 37°C. **(B)** Relative mRNA expression of *Hsp83*, *Hsp22*, *Hsp68*, and *Hsp70* genes under the same conditions. Transcript levels were quantified using the Applied Biosystems™ qPCR analysis module in conjunction with a QuantStudio™ 5 thermocycler. Fold changes were calculated using the ΔΔCt method, normalized to non-heat-shocked control cells (N) and a panel of endogenous reference genes (*18S*, *28S*, *Tub84B*, *Act5C*). Error bars represent the standard deviation from three independent biological replicates. Statistical significance was assessed using the unpaired two-tailed t-Student test. A dotted line indicates a 2-fold change threshold on the graph.

#*Note:* In Panel A, *LamC* transcripts were detected in S2 cells at approximately the 31st qPCR cycle, about 7 cycles later than in Kc cells, indicating very low expression. This correlates with undetectable level of lamin C protein in S2 cells under these conditions, as assessed by Western blot staining.

**(C)** Changes in total protein levels after heat shock induction in Kc cells. Representative Western blot images and corresponding densitometric quantification are shown for Top2, total lamin Dm, Hsf, HDAC1, lamin C, and nonphosphorylated lamin Dm at serine 25 (S25), designated ADL84 (based on antibody specificity). Images for Hsp70 are included as a heat shock (HS) indicator, and α-Tubulin is shown as the loading control. Protein levels were analyzed under four conditions: control (N), heat shock (HS), recovery (R, after 72 h), and time-matched control without HS (NR, 72 h). Densitometry values were normalized first to α-Tubulin and then to the mean intensity value of the biological replicate. Statistical significance between conditions was assessed using ordinary one-way ANOVA ($p < 0.05$), and significant differences are indicated on the graphs.

**(D)** Changes in total protein levels after heat shock induction in S2 cells. Representative Western blot images and corresponding densitometry quantification are shown for Top2, total lamin Dm, Hsf, HDAC1 and nonphosphorylated lamin Dm at serine 25 (S25), designated ADL84. Images for Hsp70 are included as a heat shock (HS) indicator, and α-Tubulin is shown as the loading control. Protein levels were analyzed under four conditions: control (N), heat shock (HS), recovery (R, after 48 h), and time-matched control without HS (NR, 48 h). Densitometric values were normalized first to α-Tubulin and then to the mean intensity value of the biological replicate. Statistical significance between conditions was assessed using ordinary one-way ANOVA ($p < 0.05$), and significant differences are indicated on the graphs.

**(E)** Western blot densitometry analysis of total lamin Dm and unphosphorylated lamin Dm at serine 25 (S25) in Kc and S2 cells. The effect of heat shock on lamin Dm phosphorylation was assessed using ADL84 antibodies specific for the nonphosphorylated form together with rabbit affinity purified anti total lamin Dm

antibodies (Lam Dm total). Western blot analysis revealed a reversible decrease in the signal for unphosphorylated lamin Dm after 1 hour of HS, while the total pool of lamin Dm (including both $Dm_1$ and $Dm_2$ forms) remained stable. Densitometry quantification was performed on three biological replicates (technical replicates: total lamin Dm — Kc: n = 14, S2: n = 11; ADL84 — Kc: n = 12, S2: n = 12). Statistical analysis using Student's t-test showed a significant decrease in unphosphorylated lamin Dm after HS compared to control (Kc: $p \leq 0.0001$; S2: $p < 0.015$), with no significant change in total lamin Dm. Densitometric values were normalized to α-Tubulin and to the mean intensity value of the biological replicate.
**(F)** Immunofluorescence analysis of nonphosphorylated lamin Dm at serine 25 (S25) in Kc cells following 1-hour heat shock at 37°C. Using ADL84 antibodies, a decrease in fluorescence signal was observed post-treatment, indicating reduced levels of the nonphosphorylated form of lamin Dm. This supports the Western blot findings and suggests increased phosphorylation of lamin Dm at S25 in response to heat stress. Both images represent Kc cells stained with DAPI (blue) for nuclei. In the left image, Top2 is shown in green and ADL84 in red, and merged overlay. In the right image, total lamin Dm is shown in green and ADL84 in red, and merged overlay. Images were acquired using confocal microscopy.

**Figure 3**
**Analysis of the distributions of Top2, lamin Dm, lamin C and DNA in Kc cells and *D. melanogaster* embryos and 3rd larval stage in normal conditions and after induction of heat shock.**
Immunofluorescence staining of Kc cells (A ) and *D. melanogaster* embryos (B) (C), (D), shows stress-induced redistribution and phenotype change of Top2, which is reversible upon recovery. Panel F demonstrates redistribution of chromatin/DAPI (F) upon HS induction in larval polytenic nuclei; Panels E and G demonstrate statistical analyses of D and F respectively. Cells, larvae and embryos were analyzed under N, HS and R conditions. Embryos were from the stage 10-12 as detected from positive signal for lamin C presence in aenocytes. Larvae were at the 3rd stage, nuclei were polyploid with nicely stained chromatin/DAPI. Densitometry graph (when appropriate) with the line density mode view is marked with the line color identical as fluorescent label on IF.
**(A)** Immunofluorescence staining of Kc cells for Top2 (green), Hsp70 (red) and lamin Dm (white). DNA stained with DAPI (blue). Arrows point to cell nuclei with typical, single granule/speckle stained for Top2. **(B)** Immunofluorescence staining of embryos (stage10-12) for Top2 (green) and lamin Dm (red). DNA stained with DAPI (blue).
**(C)** Immunofluorescence staining of embryos (stage 10-12) for Top2 (green) and lamin C (red). DNA stained with DAPI (blue). **(D)** Immunofluorescence staining of embryos (stage 10-12) for Top2 (green) and lamin Dm (red). DNA stained with DAPI (blue). This

panel is a magnified section from Panel B immunofluorescence staining to better illustrate the phenotype. **(E)** Graph demonstrating statistical significance of Top2 relocation to sublaminar region (nuclear lamina vicinity) calculated from immunofluorescence staining for Top2 and lamin Dm in embryos.
**(F)** Typical immunofluorescence staining of 3rd larva polyploid nuclei for Top2 (green) and lamin Dm (red). DNA stained with DAPI (blue). Demonstrates two typical phenotypes of distribution of DNA/chromatin: regular and sublaminal (N and HS respectively) for calculation of statistical significance of chromatin relocation. **(G)** Graph demonstrated calculated frequencies of the particular phenotype in polyploid nuclei from immunofluorescence analyses such as in Panel B and D.
Top2 rearrangement (E) and chromatin rearrangement (G) after heat shock are presented in the graphs as normalized values (the number of counted cell nuclei marked on the graphs is n). Top2 rearrangement (E) statistics (chi-square test; p=1,9*10E-27) were calculated on the basis of the number of cell nuclei counted in *D. melanogaster* embryonic cells; chromatin rearrangement (G) was calculated on the basis of the number of cell nuclei counted in 3rd instar larval cells (chi-square test; p=6,62*10E-8). Representative staining is shown on the D graph for Top2 rearrangement and on F for chromatin rearrangement.

**Figure 4**
**Stress affects the solubility of LamDm and other nuclear proteins in Kc and S2 cells. Statistical analysis of the changes in the solubility of the LamDm, Top2, Hsf and HDAC1 under increasing salt concentrations in Kc cells (Panel A) and S2 cells (Panel B).**

Control cells and cells subjected to heat shock induction were lysed and extracted sequentially as described in Material and Methods sections using buffer with increasing concentration of NaCl. Low salt buffer contained 50 mM NaCl; Medium salt buffer contained 150 mM NaCl and high salt buffer contained 500 mM NaCl. The amount of the proteins in each fraction were calculated based on Western blots bands intensity using densitometry. Western blots were probed with antibodies for: Top2, HDAC1, HSF and tubulin as a load control. For lamin Dm visualization rabbit affinity purified antibodies were used if total fractions/forms of lamin Dm were to be detected (Lam Dm total) and mouse monoclonal ADL84 antibodies specific for non-phosphorylated S25 for detection of fraction of on phosphorylated S25 lamin Dm fraction. White bars-samples from control cells; Grey bars- samples from heat shock induced cells. Heat shock induction for 60 min at 37$^{o}$C.
The data presented in the bar graphs has been validated for the mean intensity of each band from a given membrane (see M&M section).The statistics (t-student test) on the bar graphs demonstrate the comparison of the N versus HS conditions for each fraction independently. Above each plot, the number of repetitions (usually 3 biological and 4

technical) taken for the statistical analysis is given (N). The white bars in each graph refer to normal conditions (N - 23°C), and the grey bars refer to heat shock induction (HS – 1 h, 37°C). The subsequent fractions are labelled as lysate (control), 50 mM, 150 mM and 500 mM, respectively. The data has been evaluated to identify any significant differences, and these are indicated by the following symbols: “ns” - no significance,* indicates a p value<0,05, ** indicates a p value< 0,01, *** indicates a p value<0,001, and **** indicates a p value<0,0001.

**Figure 5**

**Lamin Dm colocalization and co-immunoprecititation with Top2 protein and their increase during heat shock induction.**

**Panel A** Immunofluorescence staining for lamin Dm (ADL67, top left and ADL84 top right) or lamin C (ALC28, bottom left) (red) and Top2 (green) in control conditions in 3rd instar larval tissues. DNA stained with DAPI (blue). For polyploid and polytenic nuclei visualization only merged channels are shown. Bottom, right panels: immunofluorescence staining for diploid cells, split channels with lamin Dm staining (ADL67)(red) and Top2 protein (rabbit polyclonal, affinity purified) (green).

**Panel B** Proximity Ligation Assay (PLA) analyses for colocalization of lamin Dm and Top2 in Kc cells (upper panels) and 3rd instar larvae polytenic nuclei of salivary glands (bottom panels). DNA was stained with DAPI. From left to right on both levels: control for anti lamin Dm antibody, control for anti Top2 antibody and PLA signal from both antibodies staining (red) indicates colocalization of proteins. Please see Supplemental Movies for 3D distribution of PLA colocalization signals of lamin Dm and Top2.

**Panel C** Proximity Ligation Assay for lamin Dm and Top2 proteins in 3rd instar larvae imaginal discs with the same antibodies as in Panel B. Control larva PLA staining on the left and heat shock induced larva PLA on the right. DNA stained with DAPI.

**Panel D and E** Western blot analysis of immunoprecipitation of lamin Dm and anti Top2 from Kc cells extracts prepared under native conditions as described in Materials and Methods section. In Panel E, after IP procedure additional nuclease treatment in beads, and washing steps were added to demonstrate nuclease insensitivity of the co-IP protein. Membrane was divided and stained for lamin Dm with mouse ADL67 antibody (top panel) and for Top2 with rabbit AP purified anti Top2 antibodies (bottom panel). Input-extract sample stained with antibody for lamin Dm or Top2; co-IP-immunoprecipitation anti lamin (or anti Top2) with detected binding (co-IP) partner protein. **(E)** Western blot experiment for additional nuclease in beads treatment and additional washing steps before gel loading.

**Panel F and G** Western blot analyses of the immunoprecipitation of lamin Dm and Top2 proteins from control (N) Kc cells and Kc cells with induced heat shock effect (HS). Kc

cells were fixed with PFA and extracted under denaturing conditions to ensure efficiency of extractions of major fraction of lamins and Top2 without losing their interaction partners. **Panel G** represents magnification of the part of western blot from **F**. Immunoprecipitation was performed with AP rabbit antibodies for lamin Dm and Top2. Membrane was divided and each strip processed for visualization of signal with the same rabbit antibodies as used for IP. Please note different ratio of both lamin Dm forms in normal Kc cells and heat shocked cells (lysate, input) and the same ratio retained in IP anti lamin Dm (**G**) and as co-IP fraction in anti Top2 immunoprecipitation. Please also note increased bands of co-immunoprecipitated lamin Dm and Top2 from heat shocked Kc cells.
**Panel H and I** Proximity Ligation Assay (PLA) analyses for colocalization of lamin Dm and Top2 in control Kc cells and Kc cells with induced heat shock (H), and statistical analyses of induction of additional PLA colocalization signals/loci in heat shocked Kc cells (HS) comparing to control cells (N). Statistical analysis of the Kc PLA (Panel I) revealed a significant increase in PLA signal upon heat shock. Quantification was performed on Kc cells, with approximately 100 nuclei analyzed per condition, and statistical significance was determined using the two-tailed Mann–Whitney U test ($p < 0.01$) .

**Figure 6**
Control Kc cells were used alone for the experiments in A, B and D and together with heat shock induced Kc cells in C, E and F. Immunoprecipitation was with AP rabbit antibodies for lamin Dm and for Top2. Proteins visualization was typically with ADL67 for lamin Dm and with rabbit AP anti Top2 protein with appropriate secondary antibodies and different substrates for lamin Dm and Top2 specific visualization on membranes (see Materials and Methods). WB-western blot analyses; $^{32}$P- autoradiography of the nucleic acids radioactive label from labeling with $\gamma^{32}$P-ATP and PNK kinase; ½ load/load-half of the normal volume and normal volume of extract loaded onto the beads; +S7-additional S7 nuclease treatment of the beads and additional washing steps added to the procedure; +2xS7- additional, double amount of S7 nuclease with additional washing steps.
**Panel A** No radioactive labeling with Poly Nucleotide Kinase (PNK) was used in this experiment. Input-extract to be loaded onto the beads with antibodies; wash-pulled fractions washed off buffer from washing steps; control- IP with isolated IgGs from pre-immuned rabbit serum; ½ load/load-half load and normal volume of extract loaded onto the beads; +S7-additional S7 nuclease treatment of the beads and additional washing steps added to the procedure. Please note the co-IP of Top2 with lamin Dm in this procedure and full nuclease sensitivity of co-immunoprecipitated Top2 band.

**Panel B** Western blot analysis of complete crosslinking, IP, radioactive labeling procedure and with similar experimental set up as in A. Please note the co-IP of Top2 band with lamin Dm immunoprecipitation detected in WB and autoradiography and the

full sensitivity of this Top2 bands for additional nuclease treatment. Interestingly, also label associated with lamin Dm is also nuclease sensitive up to total disappearance of radioactivity associated with immunoprecipitated lamin Dm band while protein band, despite from the fact of decreasing in intensity still persists. This experiment confirms the co-IP of Top2 with lamin Dm and also confirms that in these BrdU and UV-crosslinking procedure (denaturing conditions) is fully dependent on nucleic acids presence.

**Panel C** Western blot analysis of the crosslinking and immunoprecipitation procedure on control Kc cells and cells with induced heat shock with IP anti lamin Dm and IP anti Top2. After entire procedure IP samples were treated with buffer (-/control) or with DNase 1 and RNase A in beads followed by additional washing step and autoradiography and WB analysis. Lanes 2-4: normal cells; Lanes 5-7 heat shocked cells om WB and autoradiography panel. Samples of lamin Dm IP and Top2 IP from heat shocked cells demonstrate higher level of nucleic acids associated with their protein bands but no significant changes in proportions of sensitivity of the label for DNA and RNA digestion was detected in heat shocked cells comparing to control cells.

**Panel D** Western blot analysis of the crosslinking and immunoprecipitation procedure on control Kc cells only to test efficiency of nucleic acid binding by total fraction of lamin Dm and Top2 (total) and fractions extracted with medium salt buffer (150 mM NaCl; soluble) and high salt buffer (500 mM NaCl; insoluble). Obtained data suggest that the highest efficiency in nucleic acid binding has lamin Dm and Top2 from “soluble” fraction.

**Panel E** Western blot analysis of the crosslinking and immunoprecipitation procedure on control Kc cells and cells with induced heat shock with IP anti lamin Dm and IP anti Top2. Control-control for IP; N-IP and labeling from control Kc cells; HS-IP and labeling from heat shocked cells; R- IP and labeling from heat shocked and “recovered” cells. Data indicate that heat shock transiently increased lamin Dm and Top2 association with nucleic acids.

**Panel F** Western blot analysis of the crosslinking and immunoprecipitation procedure on control Kc cells and cells with induced heat shock with IP anti lamin Dm and IP anti Top2. Kc cells were fed with BrdU as in all experiments with addition (+) or not (-) of distamycin and divided into control cells (N) and heat shock cells (HS) before the entire procedure of the UV-crosslinking and labeling. All four cell population were analyzed in WB and autoradiography. For lamin Dm binding to nucleic acids in control cells we detected lower signal in cells with distamycin as well as in heat shocked cells with distamycin comparing to lack of distamycin. The inhibition of nucleic acid binding of lamin Dm by distamycin was in agreement with our earlier studies. Lack of changes suggest the same mode of DNA association in N and HS conditions.

For Top2 no changes in nucleic acids binding were detected in control cells between no distamycin and with distamycin. In heat shocked cells distamycin decreased the Top2 nucleic acid association might suggest that during heat shock increased binding to DNA was based on minor grove of DNA mostly.

**Panel G** Western blot analysis of the control experiment for BrdU and UV-crosslinking procedure. Experiment demonstrates that experimental procedures of BrdU

incorporation, incubation on ice, UV crosslinking, incubation with drugs (distamycin, chromomycin) and their combined effect does not induce stress response as judged by hsp70 staining on Western blots.

## SUPPLEMENTARY DATA

### Supplementary Figure 1

**Heat shock induction in *D. melanogaster* embryos**

The efficiency of heat shock induction and recovery was examined via immunofluorescence staining of *D. melanogaster* embryos under different conditions: normal, heat shock (1 h) and recovery. Merge, chromatin (DAPI - blue), lamin Dm (Lam Dm - red), and heat shock induction (Hsp70 - green) visualization.

### Supplementary Figure 2

**Assessment of gene stability after heat shock induction in *Drosophila melanogaster* cells (Kc and S2) after 1 h of HS.**

Gene expression of all tested genes (names given on the x-axis) in Kc and S2 cells (A). Bars represent the fold change in the transcript level after 1 h of heat shock induction for Kc (black) and S2 (gray). Only normalization to the control (N) was used without further normalization to the housekeeping genes. The threshold marked by a dotted line was set as 2-fold. Determination of the most stable reference (housekeeping) genes from a set of tested candidate reference genes was performed via the geNorm algorithm (B). The average expression stability was measured to choose the common endogenous control for the Kc and S2 cell lines upon heat shock.

### Supplementary Figure 3

**Immunofluorescence analysis of the distribution of nuclear proteins in Kc cells.**

Immunofluorescence staining in Kc cells; control cells (N), heat shock induced cells (HS) and recovery (R). Immunofluorescence staining for HSF, HDAC1, LBR and RNA Polymerase 2 pS5 ( all green) and Hsp90 and lamin Dm (all red). DNA stained with DAPI (blue). Please note the expected, transient relocation of Hsp90 protein to the cell nuclei of Kc cells in HS and concomitant relocation of HSF protein to the cell nuclei in HS. No other significant changes have been detected. Scale bars = 5 µm.

### Supplementary Figure 4

**Immunofluorescence analysis of the distribution of other nuclear proteins in D. melanogaster embryos.**

Immunofluorescence staining of *D. melanogaster* embryos under N, HS (1 h) and R conditions with additional fluorescence intensity analysis (A-D). Distribution of HP1 (A – red), Pol2PS5 (B - green), HSF (C - green) and HDAC1 (D – green; DNA was stained with DAPI (blue); lamin Dm (A)– green, (B-D)- red. was visualized. The area from which the fluorescence intensity was analyzed is marked with a yellow line in the “Profile”

column on each graph. A graph of the fluorescence intensity distribution (Signal intensity) for each channel is also presented (for each staining separately in the corresponding color). No significant redistribution was observed under the examined conditions. Scale bars = 5 μm.

**Supplementary Figure 5**
**Western blot analysis of the solubility of proteins in Kc and S2 control cells and after heat shock induction.**
Typical western blot from experiments for Figure 4 was shown. Panel A-Kc cells; Panel B-S2 cells. The experiment was conducted in the same way as in Figure 4. The solubility tests were performed for Hsp70, lamin Dm (total lamin Dm fraction AP rabbit Ab anti lamin Dm), lamin Dm unphosphorylated on S25 (with ADL84), Top2, HDAC1, HSF and αTub as a loading/normalization control. Please note nicely visible both forms of lamin Dm: $Dm_1$ and $Dm_2$ in extracts and less visible/resolved in lysate fractions and nice correlation of increase of upper, lamin $Dm_2$ form in extracts from heat shocked Kc and less pronounced in S2 cells (A and B). Please note the increase of lamin Dm single band staining with ADL84 antibodies in control extract (50 mM NaCl) from control Kc cells indicated increased level of lamin $Dm_1$ form in this extract (as in Figure 4A (ADL84).

**Supplementary Table 1**
**List of the primers used for RT–qPCR analysis**
Table with a list of all primers used in the RT–qPCR analyses. Their sequences, efficiency and source.

**Figure 1**

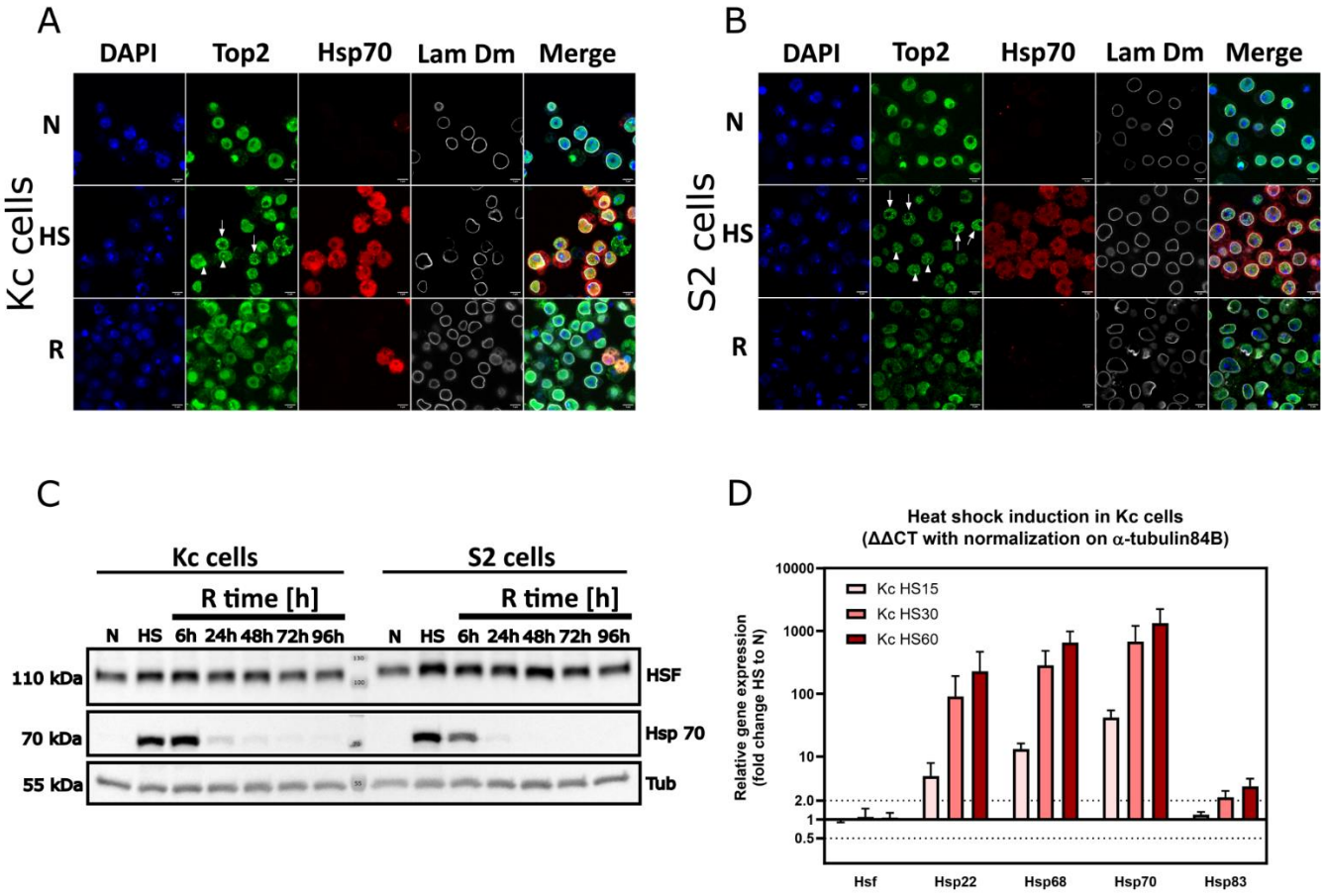
A
DAPI
Top2
Hsp70
Lam Dm
Merge
N
HS
R
Kc cells
B
DAPI
Top2
Hsp70
Lam Dm
Merge
N
HS
R
S2 cells
C
Kc cells
S2 cells
R time [h]
R time [h]
N HS 6h 24h 48h 72h 96h
N HS 6h 24h 48h 72h 96h
110 kDa
70 kDa
55 kDa
HSF
Hsp 70
Tub
D
Heat shock induction in Kc cells
(ΔΔCT with normalization on α-tubulin84B)
Kc HS15
Kc HS30
Kc HS60
Relative gene expression
(fold change HS to N)
10000
1000
100
10
2.0
1
0.5
Hsf
Hsp22
Hsp68
Hsp70
Hsp83

Figure 2

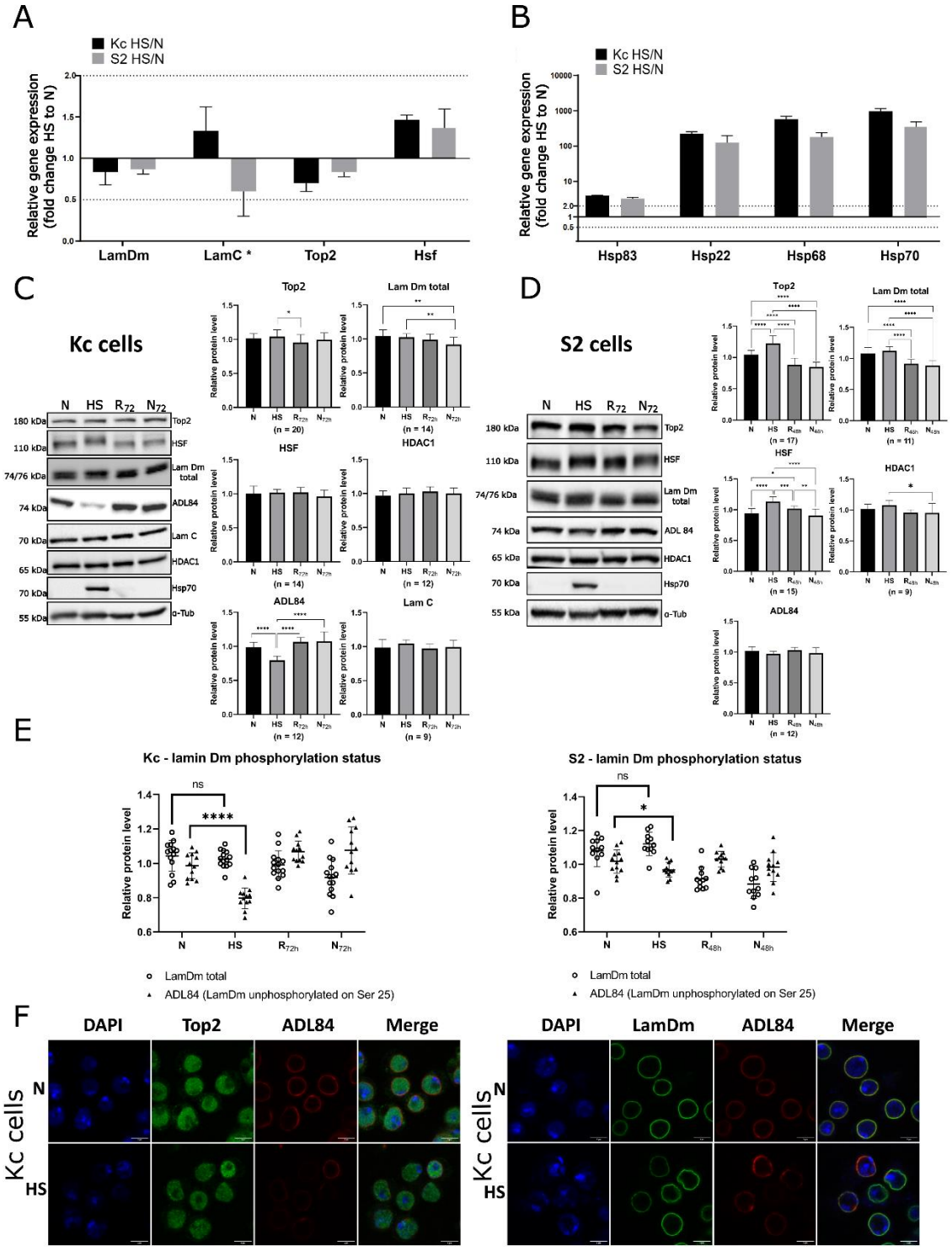
A
Kc HS/N
S2 HS/N
Relative gene expression (fold change HS to N)
LamDm
LamC *
Top2
Hsf
B
Kc HS/N
S2 HS/N
Relative gene expression (fold change HS to N)
Hsp83
Hsp22
Hsp68
Hsp70
C
Kc cells
N HS R72 N72
180 kDa Top2
110 kDa HSF
74/76 kDa Lam Dm total
74 kDa ADL84
70 kDa Lam C
65 kDa HDAC1
70 kDa Hsp70
55 kDa α-Tub
Top2
Lam Dm total
HSF
HDAC1
ADL84
Lam C
Relative protein level
D
S2 cells
N HS R72 N72
180 kDa Top2
110 kDa HSF
74/76 kDa Lam Dm total
74 kDa ADL 84
65 kDa HDAC1
70 kDa Hsp70
55 kDa α-Tub
Top2
Lam Dm total
HSF
HDAC1
ADL84
Relative protein level
E
Kc - lamin Dm phosphorylation status
S2 - lamin Dm phosphorylation status
Relative protein level
ns
****
*
N HS R72h N72h
N HS R48h N48h
LamDm total
ADL84 (LamDm unphosphorylated on Ser 25)
F
DAPI Top2 ADL84 Merge
Kc cells N
Kc cells HS
DAPI LamDm ADL84 Merge
Kc cells N
Kc cells HS

**Figure 3**

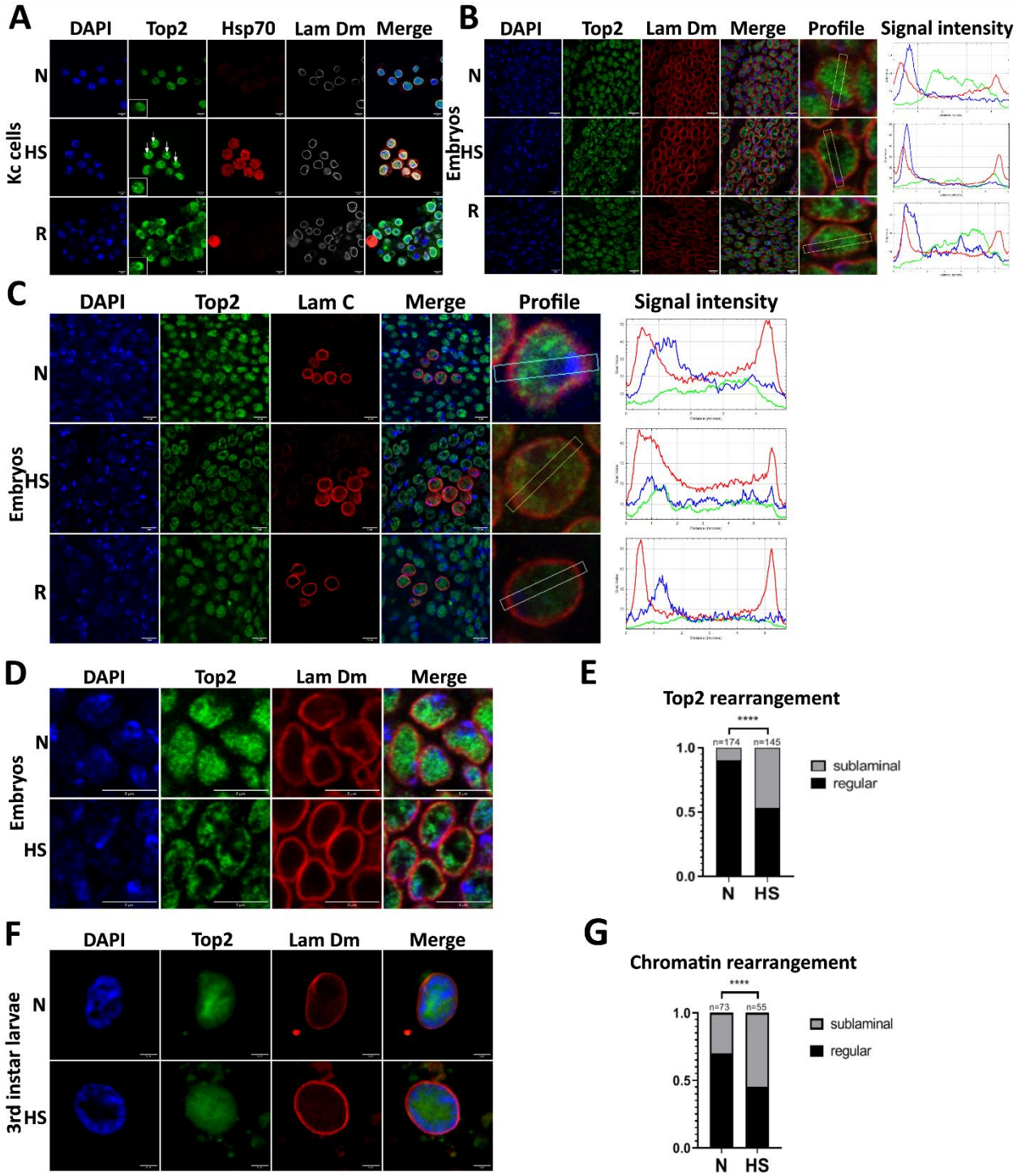
A
DAPI
Top2
Hsp70
Lam Dm
Merge
Kc cells
N
HS
R
B
DAPI
Top2
Lam Dm
Merge
Profile
Signal intensity
Embryos
N
HS
R
C
DAPI
Top2
Lam C
Merge
Profile
Signal intensity
Embryos
N
HS
R
D
DAPI
Top2
Lam Dm
Merge
Embryos
N
HS
E
Top2 rearrangement
****
n=174
n=145
1.0
0.5
0.0
N
HS
sublaminal
regular
F
DAPI
Top2
Lam Dm
Merge
3rd instar larvae
N
HS
G
Chromatin rearrangement
****
n=73
n=55
1.0
0.5
0.0
N
HS
sublaminal
regular

## Figure 4

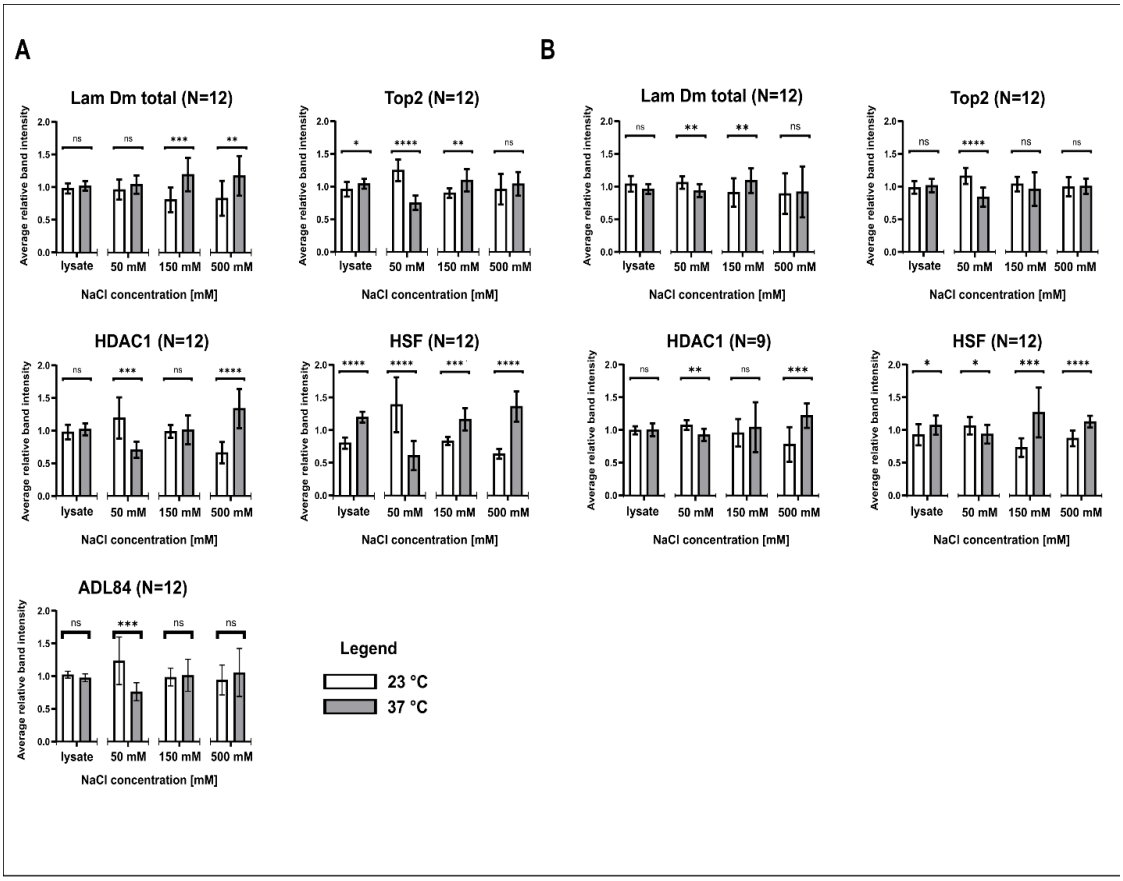
A
B
Lam Dm total (N=12)
Top2 (N=12)
HDAC1 (N=12)
HSF (N=12)
ADL84 (N=12)
Lam Dm total (N=12)
Top2 (N=12)
HDAC1 (N=9)
HSF (N=12)
Average relative band intensity
NaCl concentration [mM]
lysate
50 mM
150 mM
500 mM
Legend
23 °C
37 °C

**Figure 5**

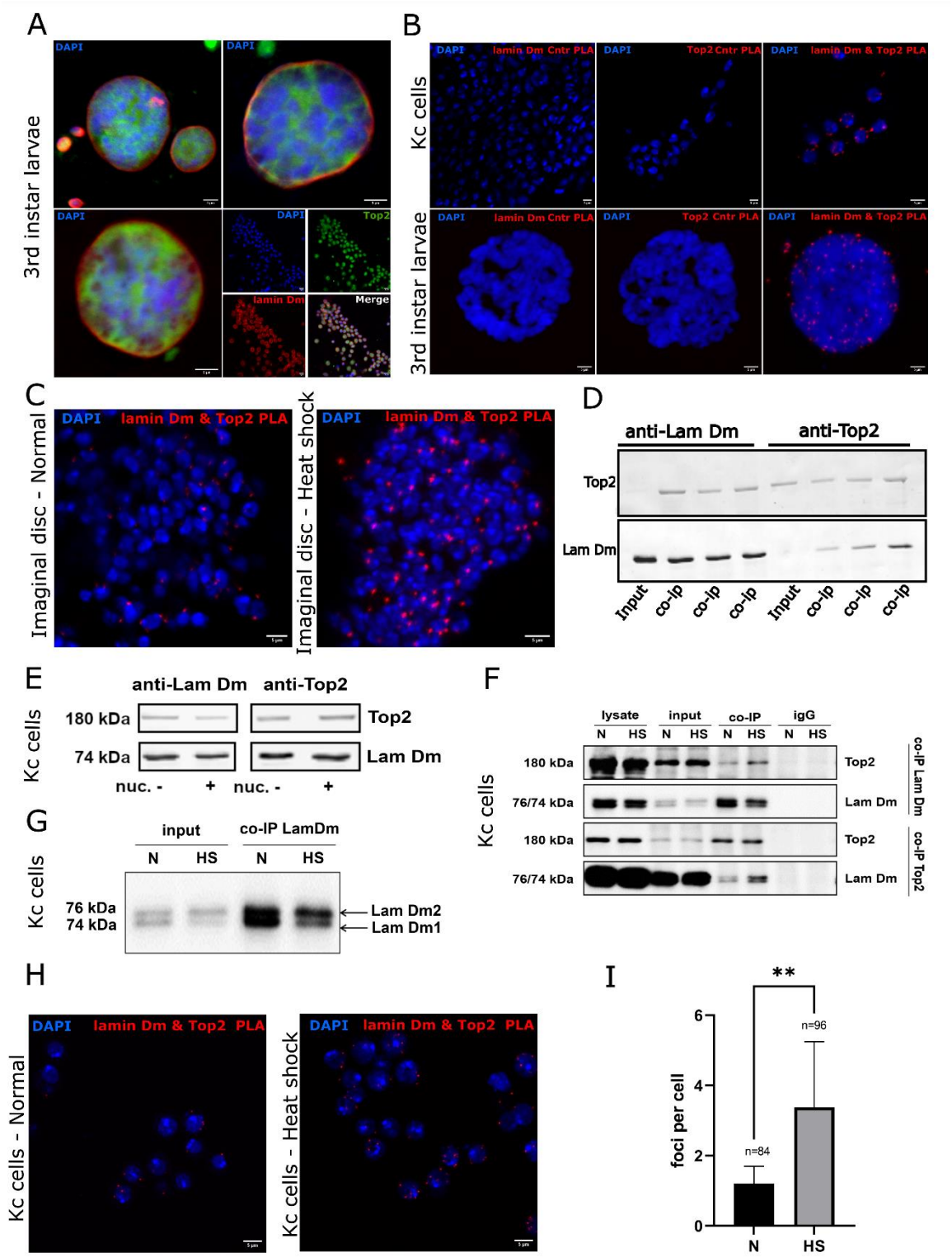
A
3rd instar larvae
DAPI
Top2
lamin Dm
Merge
B
Kc cells
3rd instar larvae
DAPI
lamin Dm Cntr PLA
Top2 Cntr PLA
lamin Dm & Top2 PLA
C
Imaginal disc - Normal
Imaginal disc - Heat shock
lamin Dm & Top2 PLA
D
anti-Lam Dm
anti-Top2
Top2
Lam Dm
Input
co-Ip
E
anti-Lam Dm
anti-Top2
Kc cells
180 kDa
74 kDa
Top2
Lam Dm
nuc. -
+
F
lysate
input
co-IP
igG
N
HS
Kc cells
180 kDa
76/74 kDa
Top2
Lam Dm
co-IP Lam Dm
co-IP Top2
G
input
co-IP LamDm
Kc cells
76 kDa
74 kDa
Lam Dm2
Lam Dm1
H
Kc cells - Normal
Kc cells - Heat shock
lamin Dm & Top2 PLA
I
**
foci per cell
n=84
n=96
N
HS

**Figure 6**

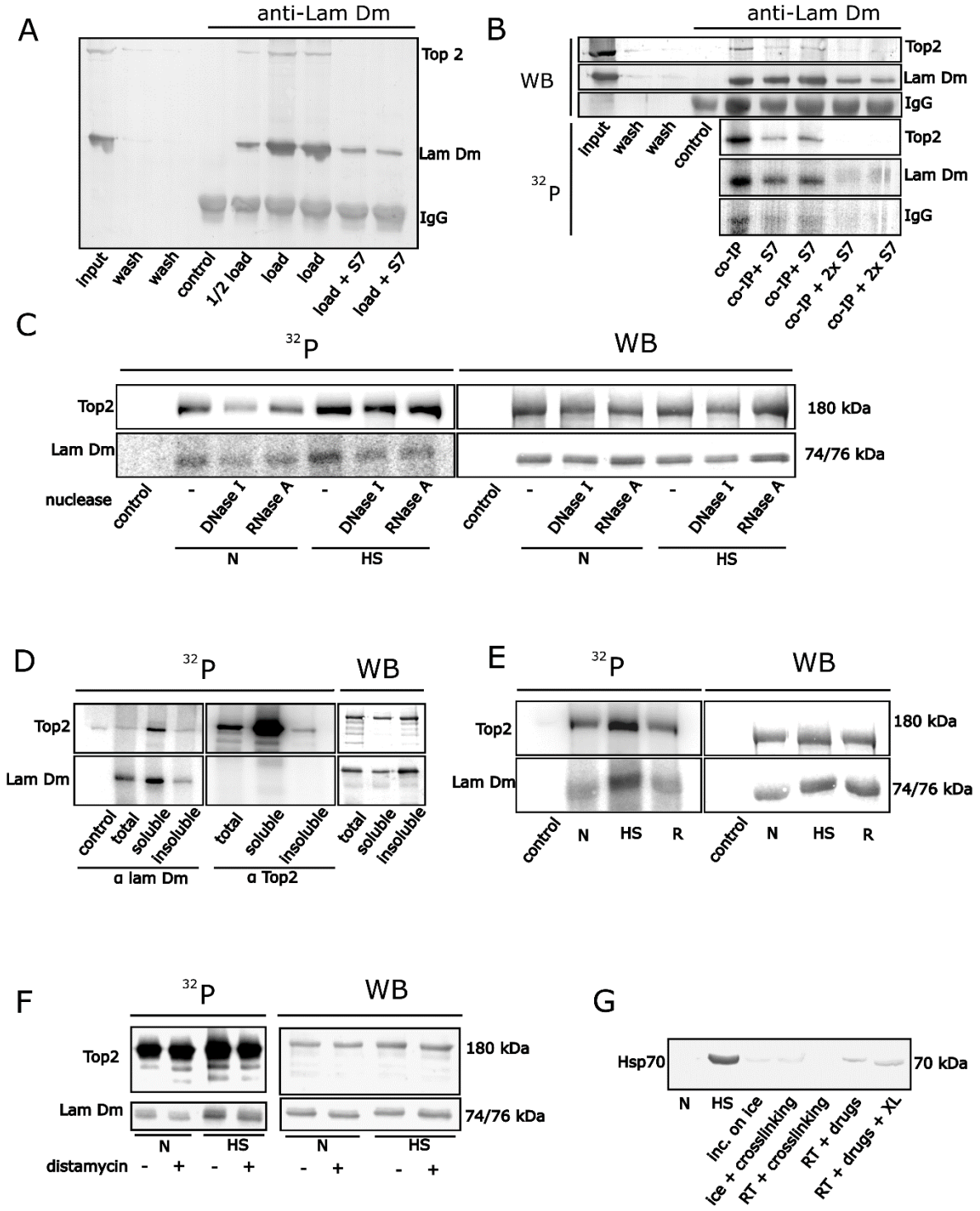
A
anti-Lam Dm
Top 2
Lam Dm
IgG
input
wash
wash
control
1/2 load
load
load
load + S7
load + S7
B
anti-Lam Dm
WB
Top2
Lam Dm
IgG
32P
input
wash
wash
control
Top2
Lam Dm
IgG
co-IP
co-IP+ S7
co-IP+ S7
co-IP + 2x S7
co-IP + 2x S7
C
32P
WB
Top2
Lam Dm
180 kDa
74/76 kDa
nuclease
control
-
DNase I
RNase A
-
DNase I
RNase A
control
-
DNase I
RNase A
-
DNase I
RNase A
N
HS
N
HS
D
32P
WB
Top2
Lam Dm
control
total
soluble
insoluble
total
soluble
insoluble
total
soluble
insoluble
α lam Dm
α Top2
E
32P
WB
Top2
Lam Dm
180 kDa
74/76 kDa
control
N
HS
R
control
N
HS
R
F
32P
WB
Top2
Lam Dm
180 kDa
74/76 kDa
N
HS
N
HS
distamycin
-
+
-
+
-
+
-
+
G
Hsp70
70 kDa
N
HS
inc. on ice
ice + crosslinking
RT + crosslinking
RT + drugs
RT + drugs + XL

**Suplementary Figure 1**

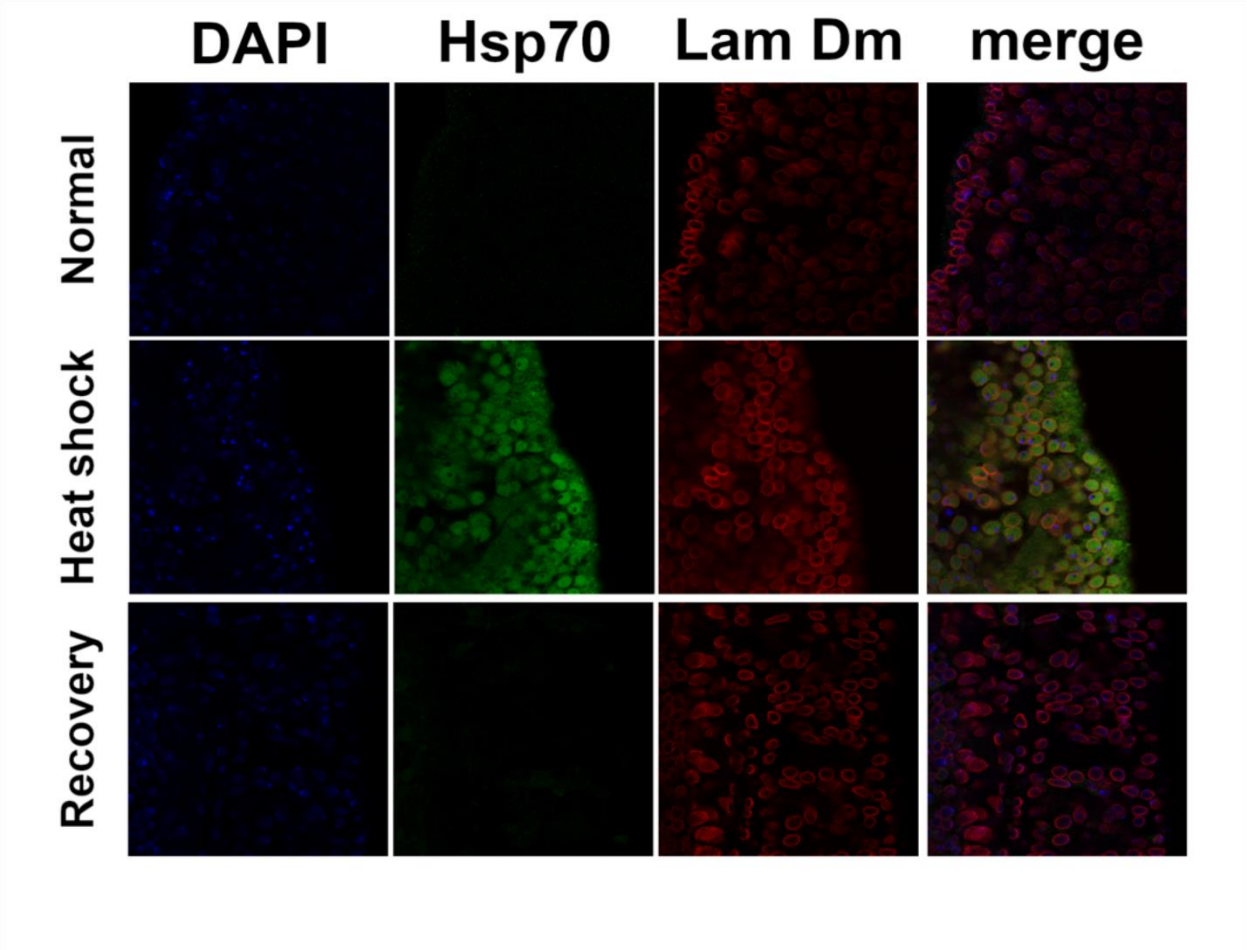

**Suplementary Figure 2**

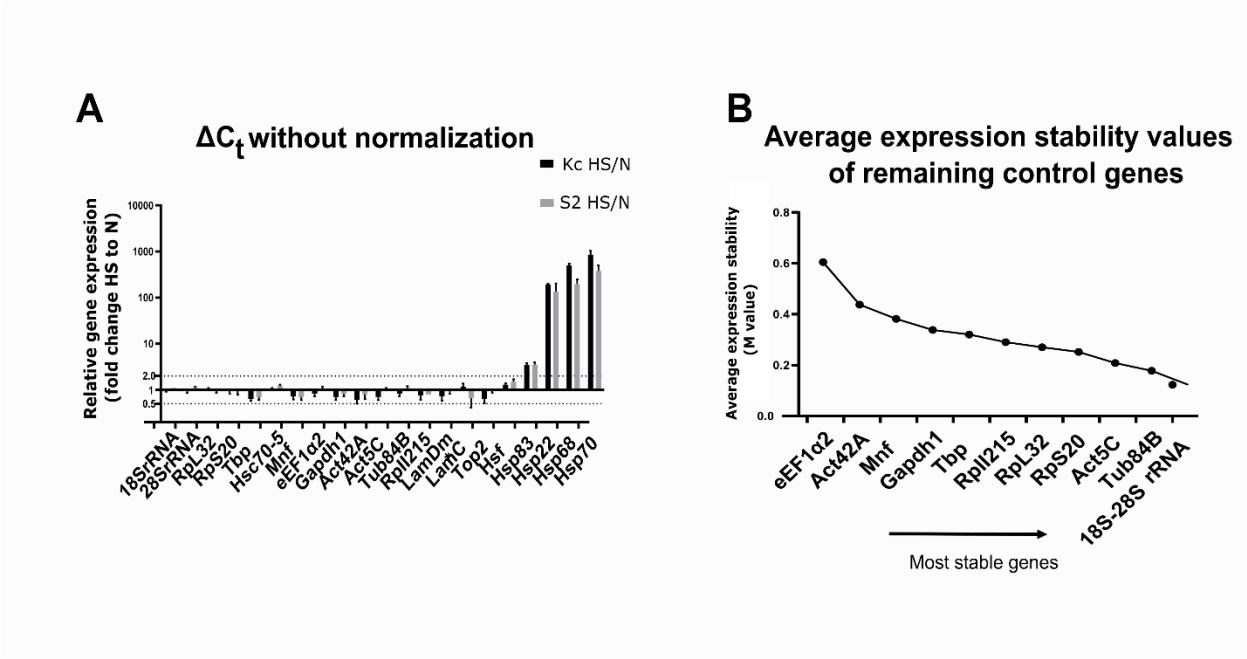

**Suplementary Figure 3**

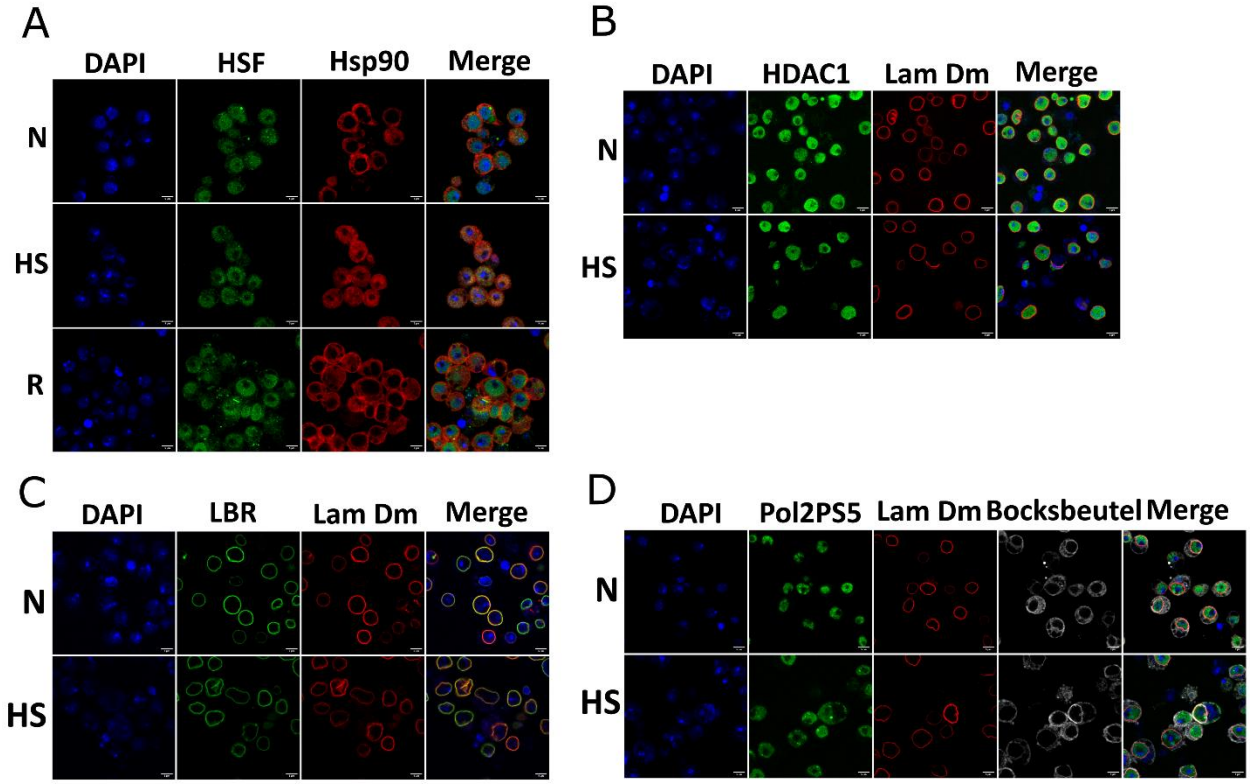

## Suplementary Figure 4

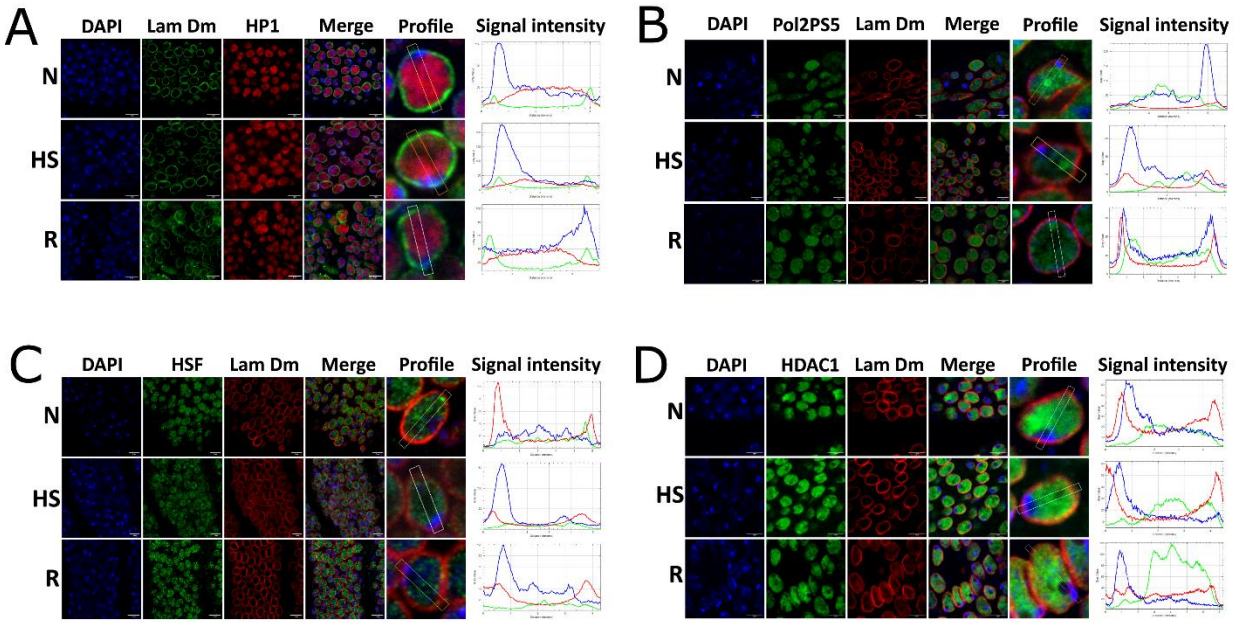

**Suplementary Figure 5**

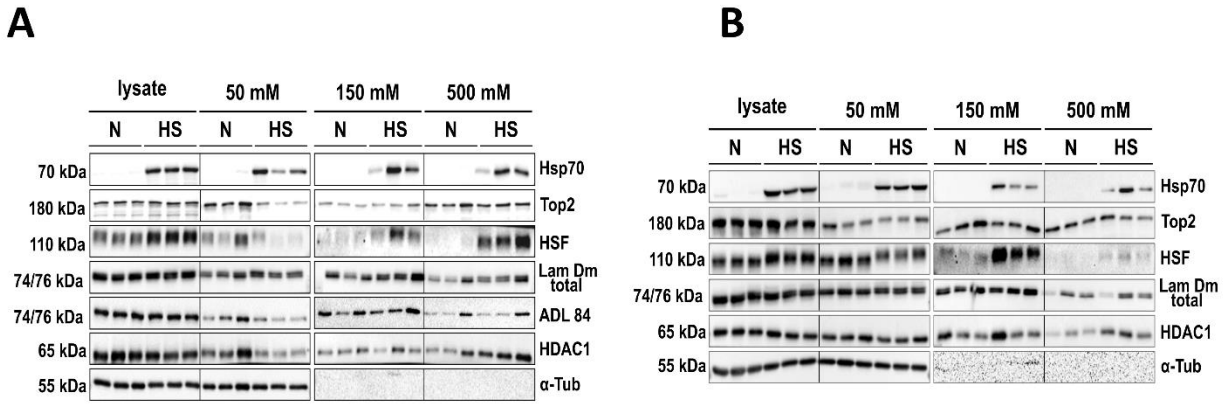

## Suplementary Table 1

Figure 2 - Figure Supplement 2 - List of the primers used for RT-qPCR analysis

| | Primer pair name | Gene name | Forward/reverse primer sequence 5'->3' | Amplicon length (bp) | Reaction efficiency (%) | Source or reference |
|---|---|---|---|---|---|---|
| 1 | 18S | 18S ribosomal RNA | F: GCCTGAGAAACGGCTACCAC<br>R: GGCCTCGGATATGAGTCCTG | 112 | 97,9 | this paper |
| 2 | 28S | 28S ribosomal RNA | F: GACGTCGCTTTTTGATCCTTCG<br>R: CGGTCTAAACCCAGCTCACG | 111 | 105,1 | this paper |
| 3 | Act42A | Actin at 42A | F: GTCATTGTGCTAAGTGTGTGC<br>R: AGCTGCAACCTCTTCGTCAC | 108 | 102,7 | this paper |
| 4 | Act5C | Actin at 5C | F: ACCAAATCTTACAAAATGTGTGACG<br>R: ACAATCGATGGGAAGACGGC | 122 | 100,8 | this paper |
| 5 | eEF1α2 | Eukaryotic translation elongation factor 1 alpha 2 | F: CAACCTGGTCACCGAAGTAAAG<br>R: CACAATCACCTGAGCGGTAAAG | 190 | 92,5 | this paper |
| 6 | Gapdh1 | Glyceraldehyde 3 phosphate dehydrogenase 1 | F: TAAATTCGACTCGACTCACGGT<br>R: CTCCACCACATACTCGGCTC | 151 | 100,3 | Hu, 2013 |
| 7 | Hsc70-5 | Heat shock protein 70 cognate 5 | F: GAATACGCAACGGCTGACAAGC<br>R: TAGCTTCTCGCACTCCTCAGC | 135 | 98,9 | this paper |
| 8 | Hsf | Heat shock factor | F: CAGTGAAAAGAAAGCACCCAGTG<br>R: GGCCTCCTGGTCATTGTTGC | 106 | 98,7 | this paper |
| 9 | Hsp22 | Heat shock protein 22 | F: TCAGTGTGCCCAATCCTCCAG<br>R: CTGGCGGCTTTGTCATTTGGC | 118 | 108,2 | this paper |

1